Université Côte d'Azur

Master MARRES

Grand Château, 28 Avenue de Valrose, 06103 Nice CEDEX 2

Characterization of dissolved organic matter in tropical estuarine sediment pore waters under ultramafic influence

Key words : Coastal sediment porewater, Photochemistry, Fluorescence spectroscopy, CDOM, Ultramafic environment, New-Caledonia

[Year 2021-2022]

Mouras Naïna

Internship from 10/01/2022 to 06/07/2022
Supervised by **Mr LEMONNIER Hugues**

Institut Français de Recherche pour l'Exploitation de la MER
101 rue Laroque
Nouméa Cedex Nouvelle-Calédonie

ACKNOWLEDGMENT

Firstly, I would like to warmly thank my supervisor Hugues Lemonnier, for this opportunity, for his support and his patience throughout my internship. Thanks to him, I had the chance to participate in almost all steps of a research project, sometimes difficult, especially for the crushing, but always instructive. Thanks also for its expertise and sharing his knowledge and giving me the wish to continue in research. But also, I thank him for his humour, his advice, and his generosity, without forgetting Cathy, for her welcome and her kindness.

A big thank you also to Florence Antypas alias "WonderFlo", for her kindness, her availability and her patience. It was an immense pleasure to be formed and guided by her. Thanks to Thomas Haize, my main labelling partner, for his contribution and help during my first analyses and fieldwork.

I would like to thank the MIO and IRD team as well as the LAMA for their significant contribution to the work on the FDOM. I would like to sincerely thank Stéphane Mounier for his precious advice for the analysis of fluorescent compounds. A big thank you to Roland Redon for setting up a new version of the ProgMEEF software. Thank you to Benjamin Oursel for his support during the crushing lab. I do not forget Cécile Dupouy, who allowed me to use the spectrofluorometer, thank you ! Thank you also to Ricardo Rodolfo for welcoming me and giving me a place in his lab, and to Cinzia Alessi for showing me her work on corals and for sharing her lab.

A special thought to the ECOMINE team (Hugues, Flo, Thomas, Raffaele, Mathisse and Dominique Ansquer without forgetting all the skippers, Jordi, Richard and Christophe) for its two months in the field, I remember our first mission and our waking up at 4 am, but also fabulous memories like the surprise of seeing Manta rays between two samples. Thank you very much for the good mood, the missions would not have been as good without all this team.

I would like to sincerely thank the members Ifremer Nouméa (Thierry Jauffrais, Simon Van Wynsberge, Romain Le Gendre, Benoit Soulard, Karen Wassaumi and Solenn Jaouen) and at the St. Vincent station for their good mood, their help and their daily support. I want to thank, the team from LEMA to welcome “cosette” for the milliQ water needed for analyses. A special thought for my favourite post-docs Alexia Dubuc and Tepoe Mai for all the good times, and the setting up of the "Tuesday cakes".

Among my colleagues who contributed to the laughter, the daily good mood, and my wish to continue in research, I think of the "top" team Anne-Lou and Robin and Chloé for their good mood and their support but also for our ice cream trips!

I'd like to thank my best office mates, Mathisse Meyneng and Anna Isaia aka the "Rays team", for supporting me in ticking off the first box on the daily to do list. More than tea mates, tissues or laughter, friends. I would like to say a special thank you to my drama team Anna Isaia and Raffaele Siano for all the moments we shared and for the support we gave each other to overcome our fear and pass our diving level. These moments will remain engraved and contributed to make my internship unforgettable. Thank you, Zio Raff, for the improvised Italian lessons on the boat and for your kind advice.

A special thought for my family who supported me and did not see me much. And hi to the coco who also took part in this internship.

ABSTRACT

To characterize the dissolved organic matter (DOM) in tropical estuarine, optical properties of coloured and fluorescent matter of porewater were measured in New-Caledonia coastal ecosystem. Surface sediment pore waters were analysed in four coastal area under different ultramafic influences, strongly (VKP, South of Nouméa), few (Dumbéa) to not impacted (Ouegoa) by mining activities. Five stations in triplicate were sampled. Absorption coefficients were low in the two stations under ultramafic soil and remarkably high in Dumbéa and Ouegoa. Spectral slope and S_R ratio indicators revealed high molecular weight molecules at the Ouegoa and Dumbéa and low in VKP. Fluorescence spectroscopy and parallel factor (PARAFAC) modeling indicate that pore water is mostly composed of 4 components, which combine both autochthonous (Humic-like-mangrove C1, Tryptophane-like C2) and allochthonous materials (Fulvic-acid C3, terrestrial-humic-like C4) in the whole sites. C1 was found in abundance at the Ouegoa and VKP which are strongly surrounded by mangroves. C2 had a homogeneous distribution along the sites with a higher concentration at VKP. The pseudo-concentration of compounds C3 and C4, were high for the Ouegoa and Dumbéa sites. The strong site effect could be explained by three main factors, presence of mangrove, size of the catchment areas, and geological conditions.

Keys words : Coastal sediment porewater, Photochemistry, Fluorescence spectroscopy, CDOM, Ultramafic environment, New-Caledonia

EXECUTIVE SUMMARY

Estuaries represent a unique ecosystem of mixing zone between fresh and seawater with important biological activity and external inputs. The association of these two drivers has a crucial influence on the composition of organic matter (OM) in sediments. Organic matter is the main source of carbon and energy for heterotrophic bacteria, which places it at the heart of marine biogeochemical cycles, as it is the basis of the microbial food chain. Two types of OM can be found, those produced directly in the environment, which are autochthonous (e.g. bacterial degradation), or those brought into the environment, which are allochthonous (terrigenous or oceanic inputs). Once in the coastal environment, the material is either considered particulate (POM) or dissolved (DOM), depending on its size. Due to a variety of biogeochemical processes, dynamic exchanges exist both within the organic matter compartment and between the sediment and the water column. For this reason, sediment and more precisely porewater is an important reservoir of DOM for the water column. The analysis of DOM pore waters is useful to identify biogeochemical processes and identify the composition and the origin of this matter along the land-sea continuum. The optical properties of coloured matter (CDOM) and fluorescent matter (FDOM) are among the most common methods for characterising MOD. New-Caledonian surface sediment pore waters were collected in four estuaries under different ultramafic influences, strongly (VKP, South of Nouméa), few (Dumbéa) to not impacted (Ouegoa) by mining activities and erosion processes. Spectral slope and S_R ratio revealed high molecular weight compounds at the Ouegoa and Dumbéa sites and low in VKP site. The parallel factor (PARAFAC) modeling indicates that pore water is mostly composed of 4 components of both autochthonous (Humic-like-mangrove C1, Tryptophane-like C2) and allochthonous materials (Fulvic-acid C3, terrestrial-humic-like C4). Optical and fluorescent indicators showed a site effect, which may linked to three reasons. A strong contribution of humic-like-mangrove compounds (C1) in VKP and Ouegoa suggests a first factor which is the presence of mangrove in the estuarine. Secondly, the high contribution of fulvic-acid and terrestrial-humic-like compounds both in Dumbéa and Ouegoa, seems to indicate the possible impact of catchment area and the hydrodynamic inputs. The third reason, for the site effect, would be potentially linked to the geology of the soils, in fact, the same characteristic was found for the VKP and South of Nouméa area, which was low CDOM content and high biological activity in porewater sediment.

Table of contents

LIST OF FIGURES

LIST OF TABLES

LIST OF APPENDIXES

GLOSSARY

CDOM: Chromophoric or Colored Organic Matter

COD: Dissolved Organic Matter

DOM: Dissolved Organic Matter

DU: Sampling site of Dumbéa

ECOMINE: Evolution of the microbial COmmunities at the outlets of the Mining Massifs
French: Evolutions des COmmunautés MIcrobiennes aux exutoires des Massifs MiniErs

EEMs: Excitation-Emission Matrix

Eh: Reduction potential

FDOM: Fluorescent Organic Matter

OA: Sampling site of Ouegoa

OM: Organic Matter

PARAFAC: PARalel Analysis FACtor

POM: Particulate Organic Matter

SN: Sampling station of South of Nouméa

VKP: Voh-Koné-Pouembout

1 INTRODUCTION

Estuaries are particularly crucial to coastal ecosystems, they represent a mixing zone between fresh and sea water at the river-sea interface, forming a unique ecosystem with important biological activity (Mayer et al., 1999). Quantity and quality of organic matter play a fundamental role in the biogeochemical processes and biological activity at this interface (Alongi, 1997). The OM compartment is essential for maintaining ecosystem health, but, in excess, it can lead to eutrophication of the environment (Paerl *et al.*, 1998). Indeed, according to the "one health" concept, the resulting degradation is also a source of risk for human health and more particularly for epidemics (Destoumieux-Garzón *et al*., 2018).

Figure 1 depict the organic matter cycle in estuaries. Organic Matter (OM) consists of a wide variety of organic compounds originating from a vast source. It can be allochthonous and come from terrigenous or oceanic contributions. Or it can be autochthonous and produced directly in the environment, for example by bacterial degradation. By convention, organic matter is characterised by its size, it either considered particulate (POM > 0,2-0,7 µm) or dissolved (DOM < 0,2-0,7 µm). During sedimentation processes, there is an aggregation of OM, which sometimes forms supra molecules (POM). On the contrary, DOM are formed by the dissolution of POM with the solubilisation of macro aggregates (Martias, 2018). There is a dynamic exchange between these two compartments, within the sediment and towards the water column (Burdige et al., 2004). Indeed, during the degradation phase of the organic matter (hydrolysis and fermentation) accumulated in the sediment (Gan *et al*., 2020), many organic and chemical components are then released towards the water column. Such discharge constitutes an important reservoir for the water column (Thomsen *et al.*, 2004). Specifically, DOM has a fundamental role in marine biogeochemical cycles by being the basis for the microbial food chain as it is the main source of carbon and energy for heterotrophic bacteria.

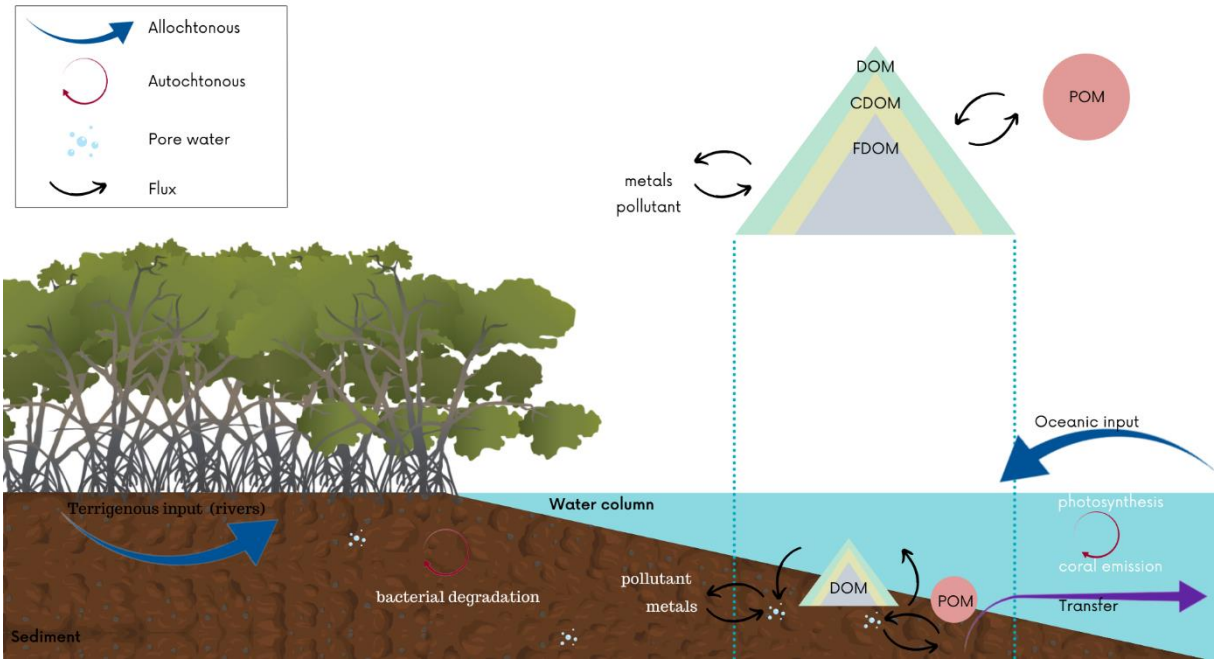

Figure 1: Organic matter at the interface zone between sediment and water column. The organic matter in coastal environments is either allochthonous (terrigenous input or oceanic input) or autochthonous (bacterial degradation, photosynthesis, or emission by corals). Within the DOM (Dissolved Organic Matter) compartment is the CDOM (Chromophoric Dissolved Organic Matter), which itself contains the FDOM (Fluorescent Dissolved Organic Matter). The DOM can contribute to the transport of dissolved metals and pollutants, through pore water. There are permanent flows between DOM and POM (Particulate Organic Matter). A large part of the organic matter is transferred between the sediment and the water column.

In recent years, the optical proprieties of dissolved organic matter have been used to identify its composition and origin in aquatic system (Tedetti *et al*., 2011). A fraction of the DOM absorbs UV radiation and visible light, it is called colored or chromophoric dissolved organic matter (CDOM) (Helms et al., 2008). It influences the colour of the ocean while participating in the attenuation of UV radiation (Coble, 2007) ; (Nelson & Siegel, 2013). Following a biological and photochemical degradation, the optical properties of CDOM are modified (Hansen et al., 2016), this modification and its analysis allows identifying the origin of DOM in ecosystems (Martias et al., 2018).

A portion of CDOM has also the characteristic to fluoresce. This part represents the Fluorescent dissolved organic matter (FDOM). Based on the fluorescence spectra obtained, the molecular structure of this portion can be determined, while the fluorescence intensity provides information on concentration (Martias, 2018).

Fewer studies on the analysis of dissolved organic matter in sediments have been conducted in the past years compared to those in the water column (Chen & Hur, 2015). Due to the important fluxes between the sediments and the water column and because sediment pore water possesses the same makers as those present in the water column, analyses of DOM pore waters are useful to identify biogeochemical processes in aquatic systems (Burdige, 2001 ; Wang *et al.*, 2013). Moreover, DOM in pore water is a helpful proxy to identify the OM sources and determine the anthropization degree of an environment (Burdige et al., 2004 ; Oliver *et al*., 2016 ; Tedetti *et al*., 2011). The major fluorophores observed in pore water sediment are Humic-like, as well as protein-like (tryptophan and tyrosine) (Burdige et al., 2004 ; Burdige, 2001 ; Otero et al., 2007). Metals can interact with DOM, a quenching phenomenon can occur affecting its fluorescence (Mounier et al., 2011 ; Gauthier et al., 1986).

Analysis of DOM in coastal sediment pore waters could be essential to improve our knowledge on the biogeochemical processes along the ultramafic land-sea continuum. In our study, four coastal areas under different geologic conditions were selected. New Caledonia was chosen as a case study because mining activity and erosion processes are targeted as the main source of metal contaminants in downstream ecosystems (Ambatsian *et al.,*1997*)*. To our knowledge, this study is innovative, as no surface organic matter sediment signatures have been defined at the interface between land and sea. The objective of this study was to analyse the composition and the origin of dissolved organic matter in sediment under ultramafic influences and to determine the presence of potential signature of ultramafic conditions. Our hypothesis is that there is a specific signature between the sites located near the ultramafic massifs, which differs from the low impacted site and the non-impacted control site.

2 MATERIAL & METHODS

2.1 CONTEXT

New Caledonia is a mountainous archipelago located in the south-western Pacific Ocean. Its unique geology is derived from the break-up of the Gondwana margin during the Late Cretaceous-Paleocene (Folcher *et al.*, 2015). More than a third of its soil is composed of ultramafic rock (Fig.2), most of which is peridotite (Folcher *et al.*, 2015). These types of rock are full of minerals (Ni, Mn, Fe, Co,) and poor in silica. For this reason, New Caledonia's economic activity is essentially based on open-pit mining of nickel, it is one of the largest reserves in the world, estimated at 20-25% (Bonvallot et al., 2013). This archipelago is surrounded by one of the largest tropical oligotrophic lagoons in the world (Benavides *et al*., 2018). In fact, a barrier reef of 1,800 km² borders the main island, called "Grande Terre" (Payri *et al*., 2018). As the second largest lagoon, after the Great Barrier Reef in Australia (Roberts et al., 2002), New Caledonia is known as a biodiversity hotspot. In 2008, the lagoon was listed as a UNESCO (United Nations Educational, Scientific and Cultural Organization) World Heritage Site. The main near-shore deposit system is influenced by terrigenous inputs (lithoclasts) which form muddy sediment within 100 m of the shoreline (Payri *et al*., 2018). Open-pit mining but also fires and several invasive species including deers contribute to deforestation, and consequently to increased soil erosion and mineral inputs to the lagoon. The lagoon waters and the coral barrier are likely to be affected by organic matter discharged by rivers, which causes trace metal dissemination (nickel, manganese, and cobalt) (Dupouy *et al.*, 2020; Martias *et al.*, 2018).

The implementation of regulations to protect and restore these hydrosystems requires their ecological status to be established and the development of health status indicators. This study is part of the ECOMINE project (Evolutions des COmmunautés MIcrobiennes aux exutoires des Massifs MiniErs) led by Ifremer, which aims to understand the impacts of mining activity on microbial communities at different time scales in order to develop biotic indicators of hydrosystem health and sanitary risks.

2.2 STUDY AREA

The New Caledonian climate is under the influence of two convergence zones: the Intertropical Convergence Zone (ITCZ), corresponding to the meteorological equator, and the South Pacific Convergence Zone (SPCZ) (Vincent, 1994). Their positions define either the warm, wet season (December to April) or the cool, dry season (June to September). The climate system is also strongly influenced by El Niño Southern Oscillation (ENSO) (Ouillon *et al*., 2010). Regarding freshwater inflows, the lagoon is provided by more than a hundred rivers. However, these inputs vary in space and time (Faure *et al.,* 2010; Fichez *et al*., 2010; Martias, 2018; Ouillon *et al*., 2010). Terrestrial inputs are abundant and amplified by multiple factors such as extreme climatic events (cyclones), erosion processes, slopes and rainfalls (Desclaux et al., 2018 ; Laganier, 1994 ; Terry & Wotling, 2011). Indeed, rivers provide many essential nutrients, including dissolved and particulate molecules in the lagoon. However, they can also carry harmful elements.

In order to identify the behaviour of DOM in New Caledonian coastal sediments, pore water samples were collected in four estuaries (Fig. 2). Two areas are highly affected by mining, one low impacted and one non impacted by ultramafic soil. The Voh-VKP-Pouembout (VKP) area is under influence of the Koniambo watersheds, and the south of Nouméa (SN) watersheds composed of Coulée and Pirogues rivers, are highly impacted by ultramafic soil. The area Dumbéa (DU) is less impacted, and finally Ouegoa (OA) with the Diahot watershed is a non-ultramafic site. For each area, five to six sampling sites (A,B,C,D,E,F) with three replicates were identified in relation with the texture of the sediment, which had to be as clayey as possible. Therefore, sixty-three sediment cores were collected

in this study. The key idea of the sampling strategy is to collect a maximum of variability, for this purpose different scales of variation are targeted: micro-scale (triplicates), the local scale between stations of the same site and finally global scale between the four sites.

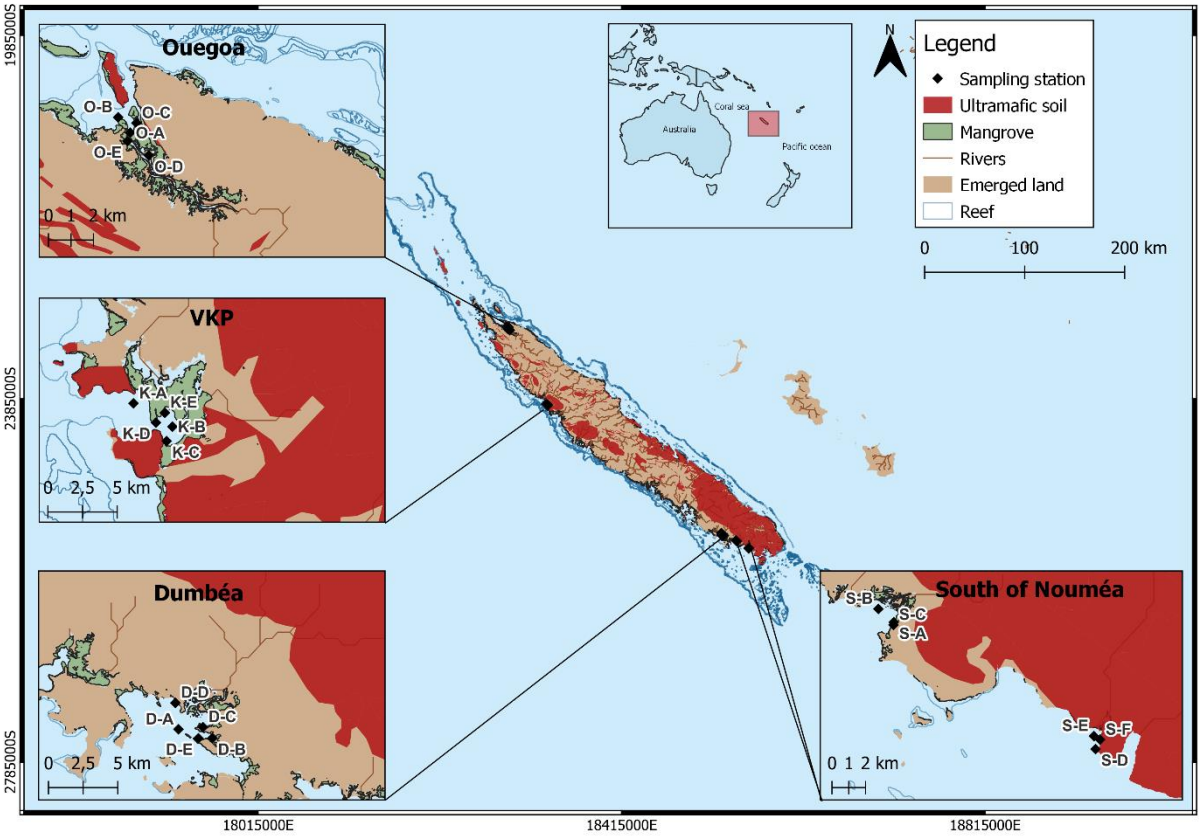

Figure 2: Map of the four sites sampled. For each site, the 5-6 stations are coded, the first letter corresponds to the site (O for Ouegoa area, K for VKP (Voh-Koné-Pouembout) area, D for Dumbéa and S for south of Nouméa) and the second letter refers to the station (A,B,C,D,E or F). Map was produced using QGIS (April 2022). All sites are under varying degree of ultramafic influence except Ouegoa.

2.2.1 Voh-Koné-Pouembout area

This VKP (Voh-Koné-Pouembout) is located in the Coco River estuary with a catchment area 260.3 km² (Lalau et al., 2019). This shallow bay is bordered by a dense mangrove swamp. Near to this area, the Koniambo massif (ultramafic) is one of the most active sites for nickel mining in New Caledonia (Perrier *et al.*, 2006). Its exploitation started at the end of the 19th century (Audet, 2009).

2.2.2 South of Nouméa area

The south of Nouméa area is composed of the Coulée and Pirogue river catchments, respectively, 84,4 km² and 147.9 km², making a total of 232.3 km² for the South Nouméa study area (Lalau et al., 2019). These rivers are located in the Grand Massif ultrabasic of South New Caledonia and carry terrestrial inputs highly concentrated in metals (Ni, Co, Mn, Cr) (Bird et al., 1984). Land-based inputs are often clearly visible after rainfall events due to their red colour and formed a mudflat (Fernandez *et al.*, 2017).

2.2.3 Dumbéa area

The dumbéa river catchment area is substantial, with 218.7 km² for Dumbéa Nord and 218.7 km² for Dumbéa Est, i.e. 437.4 km² in total (Lalau et al., 2019). This site is moderately impacted by ultramafic soil. Indeed, the ultramafic massif is not located directly at the estuary but is located upstream of the

river (Fig. 2). The estuary is bordered by a mangrove and the sedimentation of the area is composed mainly of sand, silt and clay (Fernandez *et al.*, 2017). Studies suggest that the residence time of seawater is low in dumbéa bay and the surficial sediments of the confined Dumbéa Bay are rapidly transforming (Ambatsian *et al.*, 1997).

2.2.4 Ouegoa area

Diahot River is the biggest in New-Caledonia (90 km length) (Bird *et al.*, 1984), with a catchment area of 459,9 km² (Lalau et al., 2019). This site is located at the top of the main island, with estuary surrounded by lands and extensive mangroves (Bird *et al.*, 1984) (Fig.2). The geology of Ouegoa site and more broadly the extreme north of the main island is composed of metamorphic rocks (glaucophane rocks and lawsonite schists) (Lillie, 1970). This type of rock is quartz-rich (Black, 1977).

2.3 SAMPLING STRATEGY

Sampling was taken at low tide for logistical reasons. Each campaign (collect samples and measures) was conducted on two successive days in each site. All samples were taken in 2022, the VKP was sampled in week 10, the OA in week 11, the UA in week 12 and finally the SN in week 15. For the whole ECOMINE project, six undisturbed large cores (40 cm long and 10 cm diameter) with overlying water were manually collected at each station by a diver using a manual corer to minimize sediment disturbance. Tree cores (triplicates) were used for the biological part of the study and tree cores (triplicates) for the physico-chemical part. This is illustrated in the Appendix (A1). On each core, sediment is sampled on a 3 cm thickness using a syringe cut at the tip to determine respectively the chlorophyll a content, to analyse microbial communities by eDNA metabarcoding, bacterial abundances by cytometry and meiofauna assemblages. For the chemical core, pore water was collected to analyse dissolved organic matter (DOM), dissolved metals and nutrients. Three centimeters of sediment were then collected and transferred in different storage vials to analyse total metals, sediment porosity, water content, particle size and asbestos. Within the time limit of the internship, only a part of these data will be processed in this report.

2.3.1 *In situ* sampling

Porewater is immediately extracted after coring at - 3 cm depth using soil moisture samplers Rhizon ® of 0.2 µm characterized by a vertical resolution of 1 cm, and a pressurised syringe, to avoid air contamination that causes artifacts (Fig.3) (Song *et al.*, 2003 ; Gan et al., 2020). With a single Rhizon ®, we obtained on average 10 ml of water. Even with the porosity of Rhizon being already 0.2 µm after extraction, pore water contained some remaining particles. For this reason, the water collected in the syringes was directly re-filter using a Swinnex and two overlaying burned GFF filters and then transferred into glass vials previously washed with 10% chloride acid (HLC), rinsed 3 times with Mili-Q

water and then burned (450 °C, 6 h). The samples were stored at 4°C in the dark before being quickly analysed.

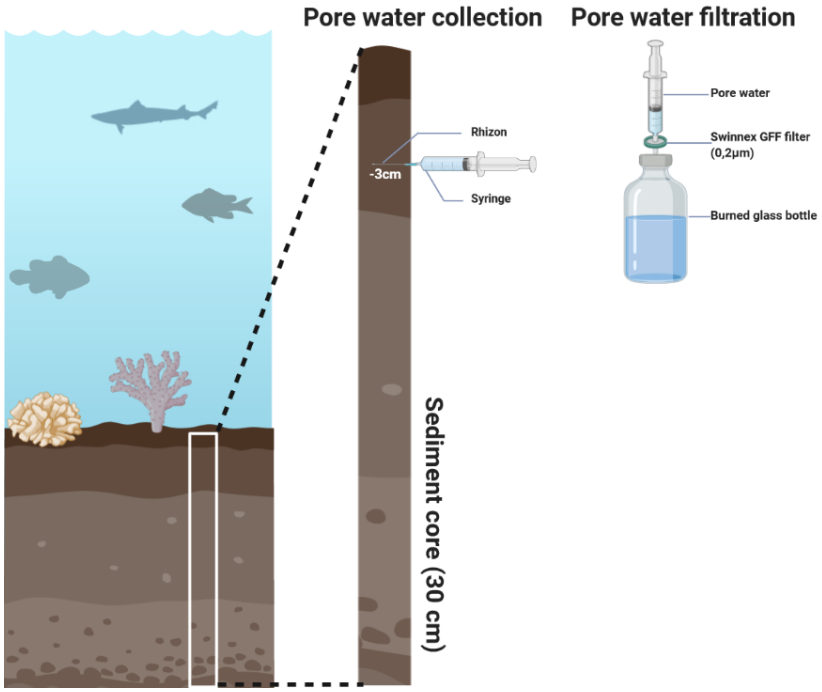

Figure 3: Sample collection and filtration of pore water sediment. Step 1 represents the sample collection on the boat and the step 2 represents the sample filtration directly from the syringe to the burned glass bottle through a Swinnex with a GFF filters (0,2)

2.3.2 *In situ* measurements

During the Rhizon extraction, the physico-chemical parameters (i.e. pH; temperature, redox potential (Eh) were measured *in situ* using several sensors. pH and Eh measurements were performed with a glass electrode 3320 WTW ® SenTix ® 81 and a SenTix ® ORD WTW ® pH315i, respectively. Measurements were made at -1.5 cm depth in the core, during at least 30 min (after a stable result). Between each sample, electrodes were carefully rinsed with sea water.

2.4 OPTICAL MEASUREMENT

2.4.1 Chromophoric dissolved organic matter (CDOM)

To characterize the CDOM, the optical properties of the material, absorption, and scattering must be considered. First, the light is absorbed by a chromatophore; this compound is part of the CDOM. When the chromophore absorbs the light, it causes the excitation of electrons, which then pass from a fundamental state to an excited state. Depending on the chemical structure of the electron, the energy required for the transition from one energy state to the other differs (Para, 2011 ; Martias, 2018). The absorption wavelengths match the energy differences between the fundamental and excited states. Based on the response at these wavelengths, the type of chromatophore can thus be characterized. In the range 200-700 nm, the absorption spectrum of CDOM evolves according to an exponential decrease (Bricaud *et al.*, 1981). The DOM can also cause scattering phenomena, by varying the refractive index.

2.4.1.1 Instrument and measures

CDOM measurements are performed at room temperature in a 1 cm quartz cell using a shimatzu UV-1700® spectrophotometer between 200 and 700 nm at a step of 1 nm. In parallel, a blank is made with milli-Q water. This system is connected to a laptop allowing acquisition of the data by Uvprobe

software. Between samples, the cell is rinsed three times with 10% HCL then 3 times with fresh Mili-Q water.

2.4.1.2 Data processing

Excel and R software version 3.6.1 allows automating the processing of CDOM spectra in 6 steps with the package CDOM that used the Gaussian decomposition method (Massicotte & Markager, 2016).

1) Extraction of the absorptions at wavelengths 250, 254, 350, 365, 442, 465, 665 nm
2) Calculation of absorption coefficients from the formula:
$$\text{Absorption coefficient (aCDOM (l))} = \frac{(2{,}303 \times \text{absorbance}(\lambda))}{\text{optical path length in m}}$$
The Factor 2.303 allows for the change from the natural logarithm to the decimal logarithm (Oliver *et al.,* 2016), (Coble, 2007).
The absorbance value a_{254} nm is used as an indicator of CDOM photodegradation (Martias, 2018). The absorption coefficient a_{442} is used as a proxy for biological production (Benavides *et al*., 2018), (Dupouy *et al*., 2020). On the contrary, the coefficient a_{350} indicates terrestrial input to the waters (Benavides *et al.,* 2018), (Dupouy *et al.,* 2020).
3) Calculation of spectral slopes ($S_{275\text{-}295}$ et $S_{350\text{-}400}$). The determination of spectral slopes values proceeds in several stages. The absorption coefficient (aCDOM(l)) logarithm is calculated along a specific wavelength range. Then a linear regression can be plotted. It is from this modelling that the slope S is calculated as well as the coefficient of determination R^2. The R^2 coefficient allows us to check the quality of the prediction of the simple linear regression. The closer the R^2 is to one, the more the dataset tightens around the linear regression line and the more the slope will be representative of the dataset. It appears that the higher the value of the spectral slope ($S_{275\text{-}295}$), the lower the molecular weight of the CDOM (Hansen et al., 2016).
4) Calculation of the SR ratio between $S_{275\text{-}295}$ and $S_{350\text{-}400}$ spectral slopes. This ratio is also related to the molecular weight as well as the photodegradation process (Helms et al., 2008) ; (Benavides et al., 2018) ; (Hansen et al., 2016). A SR ratio of less than one is more suggestive of terrestrial CDOM usually characterized by high molecular weight of DOM (Hansen et al., 2016). It will be considered of oceanic origin and/or a low molecular weight with a ratio greater than 1.5 (Helms et al., 2008).
5) Calculation of the E_2/E_3 index, which provides information on the aromaticity and molecular weight of CDOM (Hautala et al., 2000 ; Thomsen *et al*., 2002). This index is calculated with the absorbance at 250 nm divided by the absorbance value at 365nm, the smaller the ratio, the greater the aromaticity and molecular size (Rocha *et al*., 1999).
6) E_4/E_6 index refers to the absorbance 465 nm/665 nm and gives information on the molecular size and weight. This index value indicates the composition of DOM, below 5, is rather composed of humic acid while above 5, the material will be composed of fluvic acid (Abaker, 2016).

2.4.2 Fluorescence measurement

After the light absorption, the chromophore must stabilize. It can return either to the fundamental state or to an intermediate energetic state thanks to the emission of a photon, which is the fluorescence phenomenon. The chromophore is then a fluorophore. The light of fluorescence has a wavelength higher than the light of excitation (Martias, 2018). Fluorescent techniques are more sensitive than absorption spectroscopy and provide more information about the chemical composition. Fluorescence is studied by 3D spectrofluorometry with a spectrofluorometer.

Pore waters are very absorbent and may be subject to inner filtering effects and thus distortion of the spectra which causes a non-linear relationship between the intensity of fluorescence and the concentration (Otero *et al.,* 2007). In order to maintain a linear relationship between sample concentration and fluorescence intensity, the absorbance should not be greater than 0.05 cm^{-1} at 220nm (Burdige *et al*., 2004), or 0.01 cm^{-1} at 350 nm (Gan *et al.,*2020) or 0.01 cm^{-1} at 250 nm (Otero *et*

al., 2007). To avoid dilution issues, the alternative is the use of a spectrofluorometer cell with a shorter length. In our case, we chose to use an asymmetric 2 mm cell to analyse FDOM in pore waters.

2.4.2.1 Instrument and measures

Fluorescence analyses are performed with a PERKIN ELMER LS 55 spectrofluorometer at room temperature in the Marine Chemistry Laboratory at the IRD campus. The matrix is acquired for excitation wavelengths of 200–500 nm every 5 nm and for emission wavelengths of 280–550 nm every 5 nm. The exciting light source consists of a 20-kW xenon flash lamp and a Monk-Gillieson type monochromator.

Before analysis, samples were brought to room temperature (20°C) then transferred to a quartz cell of 2mm optical path, washed beforehand with 10% HCL. Before each analysis, cell was rinsed 3 times with 10% HLC, then 3 times with fresh Milli-Q water and three times with the sample if the quantity allowed. In the spectrofluorometer, the cell was maintained at 20°C by a water circulation system around the cell holder and a thermostatic bath. The asymmetric cell is set with the 2 mm side towards the excitation beam, the emission is then collected through the 1 cm optical length side.

One of the most widely used techniques is the Excitation-Emission Matrix Spectroscopy (EEMS) (Coble, 2007 ; Coble 1996). This method allows establishing a 3D map of the composition of fluorophores. The acquisition parameters of EEMs are presented in Table 1.

Table 1: Parameters of the PERKIN ELMER LS 55 spectrofluorometer used for the acquisition of EEMs

Parameters	Value
Speed	1200 nm/min
Excitation and Emission slit	5 nm
Answer time	0.5 s
Range λ_{Em}	280-550 nm
Range λ_{Ex}	200-500 nm

2.4.2.2 Data processing

EEM of 63 samples were modelled by parallel factor analysis (PARAFAC) (Bro, 1997). PARAFAC treatment requires at least nine homogeneous EEMs in terms of fluorophore composition. Several steps are needed for PARAFAC analysis, listed in Table 2.

Before interpretation, all data were normalized with the pure water Raman scatter peak at Ex/Em = 275/303 (Coble, 1996). This step allows to get rid of the Raman and Reyleigh dissolution bands, which can have intensity higher than the fluorescence peak of the fluorophores. The Raman standardization was done using the Zepp et al. (2004) method, by dividing EEM by the Raman peak.

Then EEM are decomposed in order to identify the common fluorophore. CORCONDIA (CORe CONsistency DIAgnostic) algorithm retains only the dominant fluorophore groups that are found in the majority of the samples assessed. In fact, PARAFAC calculates a percentage called CORCONDIA which allows to estimate the quality of separation of the spectral contributions. When the CORCONDIA is more than 60%, this number is chosen as the number of components (Zhao, 2011). The detected components are then compared to literature.

The parallel factor Analysis (PARAFAC) was analysed using the ProgMEEF software (Mediterranean Institute of Oceanography (MIO) – Université de Toulon, 2018) through MATLAB R2017a software. A new ProgMEEF routine was required as the samples were analysed with an asymmetric 2mm-10mm optical pathway cell. This new version was completed in April 2022 (© Roland Redon MIO Toulon).

Table 2: Parameters used in ProgMEEF for the acquisition of EEMs

Parameters	Value
Scattering correction	Method : Zepp
	Cut-off width : 25
Inner filter correction	Method : No correction
Raman correction	Method : No correction
Scaling correction	EEms scaling : None
Decomposition	Method : PARAFAC (Bro)
	Number of components Min : 2 ; Max : 5

Various fluorescence indexes such as BIX (biological index) (Parlanti et al., 2000), HIX (humification index)(McKnight et al., 2001), FI (Fluorescence index) (Zsolnay et al., 1999) are calculated from the 3D fluorescence spectra. The fluorescence indexes coupled with other water quality data can be used to characterise the source of humic materials in particular fulvic acids (McKnight et al., 2001).

2.5 SEDIMENT TYPE

In order to obtain information on the type of sediments, water content is computed. The water content is determined according to the following equation and expressed in wet weight :

$$Water\ content\ (\%) = \frac{(ww - dw) \times 100}{(ww - ew)}$$

ww: weight of box with wet sediment (g)
dw: weight of the box with dry sediment (g)
ew: empty box weight (g)

2.6 STATISTICAL STUDY

In this study, descriptive statistical, principal component analysis, correlation matrix, PERMANOVA were carried out through R software in version 4.0.3. For all analyses, it was considered that ($p > 0.05$) was not significant and ($p < 0.05$) was significant.

Statistical differences for both sites and stations were tested using the Kruskal-Wallis non-parametric test because application conditions (normality and homoscedasticity) were not satisfied. Then, when it was necessary, a pairwise multiple comparisons using the Wilcoxon test was undertaken.

Additionally, to analyse the differences either between or within sites for all optical characteristic data (i.e. a_{254}, a_{350}, a_{442}, $S_{275\text{-}295}$, $S_{350\text{-}400}$, SR) a multivariate analysis PERMANOVA was performed. We chose Euclidean dissimilarity as the association coefficient. To analyse the potential influences of factors (physico-chemical parameters, optical parameters, and fluorescence indexes and compounds) a principal component analysis (PCA) was done. Being based on the Euclidean distance, the double zero should be important to consider in the raw database especially for environmental variables. The data are heterogeneous from a unit perspective, for this reason it has been center-reduced to overcome the problems of different ranges of variation.

One of the application conditions of the PCA is the normality of data, in other case, the PCA is accepted if the number of objects is higher than the number of parameters. Moreover the PCA has been carried out with a spearman correlation matrix (non-parametric correlation matrix).

3 RESULTS

3.1 PHYSICO-CHEMICAL PARAMETERS

The mean physico-chemical parameters calculated by site are shown in Table 3 and all values are list in Table A1 in Appendix. The parameter comparison between sites is illustrated in Appendix A2.

Table 3: Mean ± standard deviation of in situ physico-chemical parameters (temperature, salinity, pH, Eh, Water content).

Site	T (°C)	Salinity	pH	Eh (mV)	Water content (%)
VKP	31,0	30,0	7,4 ± 0,15	-95 ± 54	40 ± 13
OA	30,2	28,0	7,4 ± 0,14	-73 ± 37	42 ± 12
DU	28,8	33,1	7,6 ± 0,21	-45 ± 29	40 ± 15
SN	27,7	25,6	7,6 ± 0,16	-72 ± 109	36 ± 5

The temperature ranged from 26° to 31.7°C. The lowest value was recorded in the estuary of the Coulée at SN (st A); the highest value was measured near the mouth of the Coco River at VKP (st B).

Salinity was variable at each site depending on their distance from the river and between sites. The salinity ranged from 15.0 at SN (st A) to 34.4 at DU (st A). The non-parametric statistical tests Kruskal walis and the Wilcoxon multiple comparison test allow to see that the salinity of DU is significantly different from OA ($p < 0.01$), and that SN is significantly different from DU ($p < 0.01$).

The pH measured in sediment showed a low variation range between stations, with a maximum of 7.8 recorded at DU (st C) and a minimum of 7.2 at VKP (st D). However, despite these relatively small variations, the pH measured at VKP was significantly different between stations ($p < 0.05$; Kruskal-Walis) (Fig.4.iA). A significant difference was observed between the pH conditions at SN and VKP ($p < 0.05$) (Appendix A2.iv).

Variability range for the Eh was huge [(+21 mV) to (-219 mV)], with strong differences between sites and stations. With very large standard deviations were also observed (e.g. -219 ± 160 mV at SN - station B). The differences between Eh measurements were significant between stations at OA ($p < 0.05$; Kruskal-Walis) (Fig.4.iii.B).

The water content showed a minimum of 22% at VKP (st A: 22 %) and a maximum of 60% at DU (st B). Intra-site variations for VKP, OA and DU were significant ($p < 0.05$; Kruskal-Walis) (Fig. 4.ii). The variability within the same site was such that no differences were identifiable between sites (Appendix A2. B). From a qualitative point of view, the type of sediment was rather homogeneous between the 3 sites under ultramafic influence (VKP, DU, SN) (more or less reddish and matt colour). Sediments collected at OA were rather black with shiny particles of quartz.

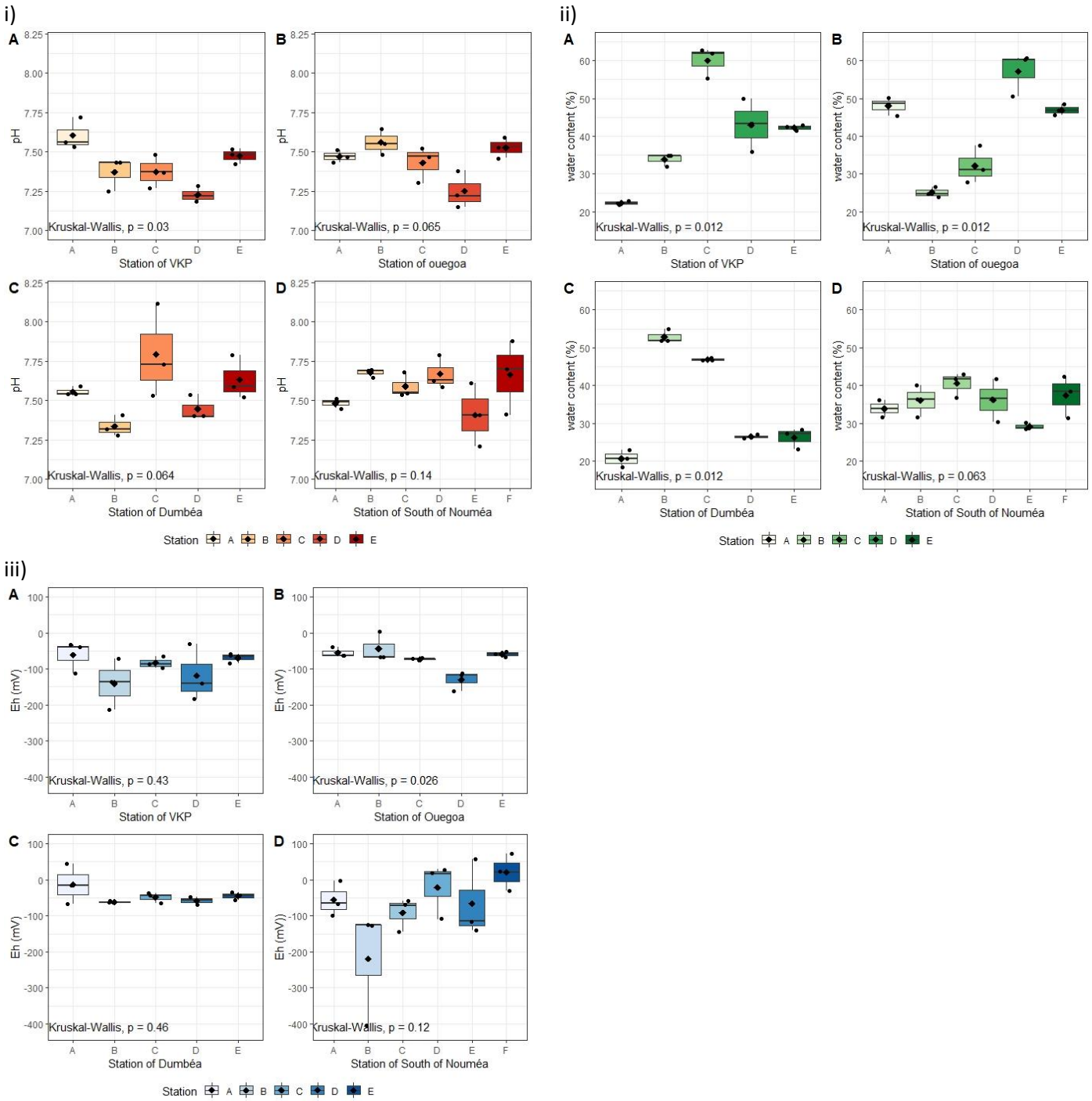

Figure 4: Box plot illustrating intra-site variability about the different physicochemical parameters measured on the 5-6 station (A,B,C,D,E,F) and the 4 sites (VKP : A, Ouegoa : B, Dumbéa : C and South of Nouméa D) during the ECOMINE Campaign (March-April 2022). i: pH in orange, ii: Eh in blue and iii: water content in green.

3.2 OPTICAL PROPERTIES OF CDOM

3.2.1 CDOM characterization

The average absorption coefficient at 350 nm, a proxy for terrigenous matter in coastal systems, varied from 11.4 ± 5.53 m^{-1} at VKP to 72.7 ± 81.4 m^{-1} at OA (Tab.4). The values obtained for the VKP, OA and DU sites showed a high degree of intra-site variability ($p < 0.05$), more than those of SN (Appendix A.3). Furthermore, when we consider the whole samples (inter-site differences) (Fig.5), we observe a significant site effect on the values of a_{350} coefficients. Indeed, the statistical analyses allow us to see

two distinct groups among the sampling sites, no significant differences were observed between SN and VKP (p = 0.54), and between DU and OA (p = 0.43).

The observations made for the a_{350} (m^{-1}) coefficient were similar to those for a_{442} (m^{-1}), a proxy for biological activity, with the highest values for OA and DU sites with 34.5 ± 38.8 m^{-1} and 22.8 ± 13.9 m^{-1}, respectively (Tab.4). The lowest values were measured for samples from the sites of VKP and SN with respectively 4.45 ± 2.88 m^{-1} and 9.13 ± 6.65 m^{-1}.

Table 4: Mean ± standard deviation of CDOM parameters (a350, a442, S275-295, S350-400, SR, E2/E3, E4/E6) determined in surface sediment pore waters from VKP, Ouegoa (OA), Dumbéa (DU) and South Nouméa (SN) during the ECOMINE campaign (March-April 2022).

	Mean and standard deviation			
	VKP	OA	DU	SN
a_{350} (m^{-1})	11.4 ± 5.53	72.7 ± 81.4	31.2 ± 20.0	14.3 ± 9.05
a_{442} (m^{-1})	4.45 ± 2.88	34.5 ± 38.8	22.8 ± 13.9	9.13 ± 6.65
$S_{275-295}$	0.015 ± 0.002	0.009 ± 0.004	0.005 ± 0.003	0.008 ± 0.005
$S_{350-400}$	0.012 ± 0.002	0.009 ± 0.003	0.003 ± 0.001	0.006 ± 0.004
S_R	1.30 ± 0.20	0,94 ± 0.34	1.77 ± 0.65	1.34 ± 0.29
E_2/E_3	3.86 ± 0.83	2.54 ± 0.88	1.53 ± 0.57	2.36 ± 1.34
E_4/E_6	3.11 ± 2.10	2.84 ± 0.53	2.35 ± 0.33	2.61 ± 0.55

The mean values of the slopes calculated between 275 and 295 nm ranged from 0.005 ± 0.003 at DU and 0.015 ± 0.002 at VKP. The spectral slope values obtained for DU and SN showed significant median variability between stations (Appendix A3). Two sites differed significantly from the other. The VKP site had more low molecular weight molecules (S significantly higher than those of the other three sites), while the DU site had significantly ($p < 0.05$) higher molecular weight molecules (lowest S) than the other three sites (Fig. 5).

The slope ratio SR, which is an indicator of molecular weight and photodegradation, was greater than 1 for VKP (1.30), DU (1,77) and SN (1,34) and < 1 for the OA (0,94) site, indicating high molecular weight terrestrial molecules for the OA site.

The indicators E2/E3 and E4/E6 are indices that estimate the size of humic substances (E2/E3) and the predominance of either humic acid or fulvic acid (E4/E6). Due to the variability within a site, it was required to consider the indices per station to better identify the type of material present in CDOM (Tab A1, Appendix). The E2/E3 indicator showed the lowest values at DU with an average value of 1.53 ± 0.57, indicating the presence of large and aromatic molecules. VKP site presented the highest values with an average of 3.86 ± 0.83, indicative of low aromaticity and small size molecules. The E4/E6 index was lower than 5 for all stations (Table. A1 Appendix) except for st B at VKP (7.00 ± 1.00), indicating a predominance of fulvic acid at this station.

In order to draw significant differences either between or within sites for all optical characteristic data (i.e. a_{254}, a_{350}, a_{442}, $S_{275-295}$, $S_{350-400}$, S_R) a multivariate analysis (PERMANOVA) was performed, which allows testing the simultaneous response of several variables to several qualitative factors. We chose Euclidean dissimilarity as the association coefficient. The qualitative explanatory factors chosen were the sites and the stations. The type of site significantly explained 28% of the dissimilarities of the samples on the basis of the CDOM indicator values ($p = 0.001$). The stations appeared to be a significant factor as they explain 68% of the dissimilarities ($p = 0.001$).

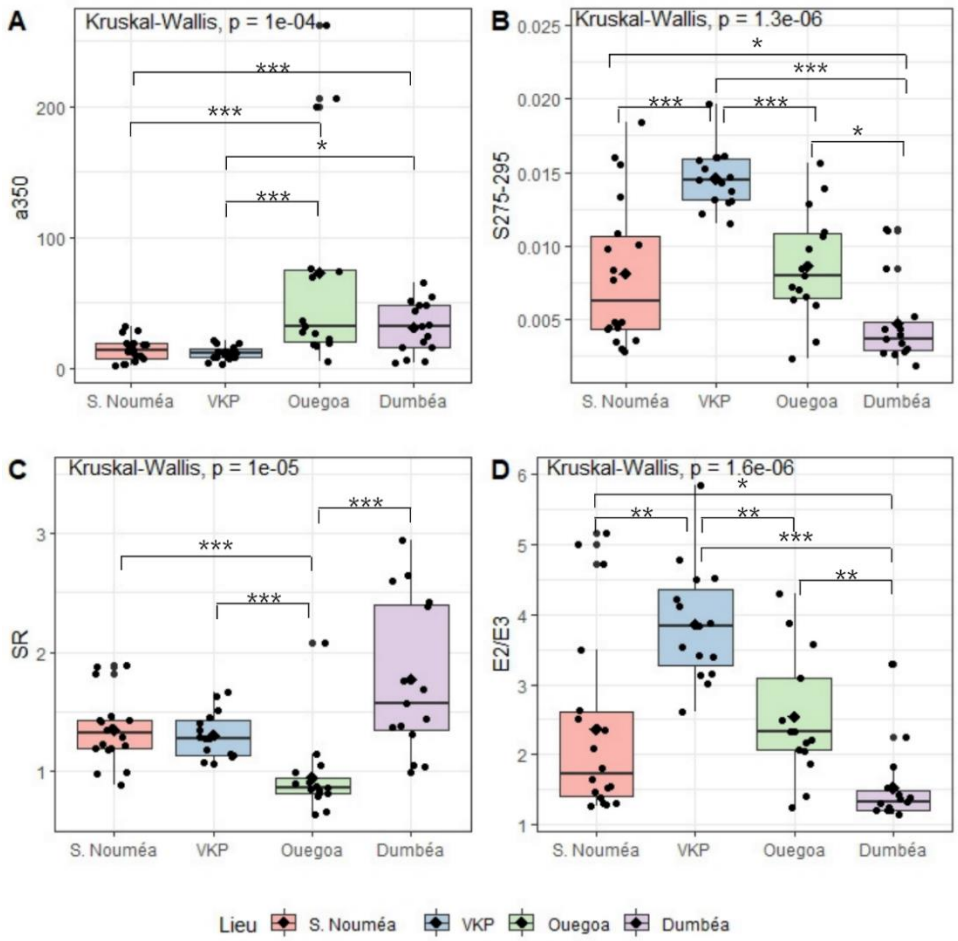

Figure 5: CDOM absorption coefficients at 350 nm (m^{-1}) (A), spectral slope $S_{275-295}$ (B) and SR slope ration (C) for each site (VKP : red, Ouegoa : blue, Dumbéa : green, South of Nouméa : Purple). The mean value is indicated by a black diamond and the median by a black bar. Significant differences are indicated by stars (: p-value < 0.05; ** p-value < 0.01; *** p-value < 0.001. Note that the ordinate axes are not the same between parameters.*

3.2.2 FDOM characterization

In order to characterise the composition of fluorophores contained in FDOMs of the sites studied, and to observe whether there was a common trend, a PARAFAC treatment was carried out on all samples. Similar compounds were identified between sites. The results of the analysis of the 63 EEMs are presented below.

The contributions of identified fluorophores are presented in Table 5 and Figure 6.

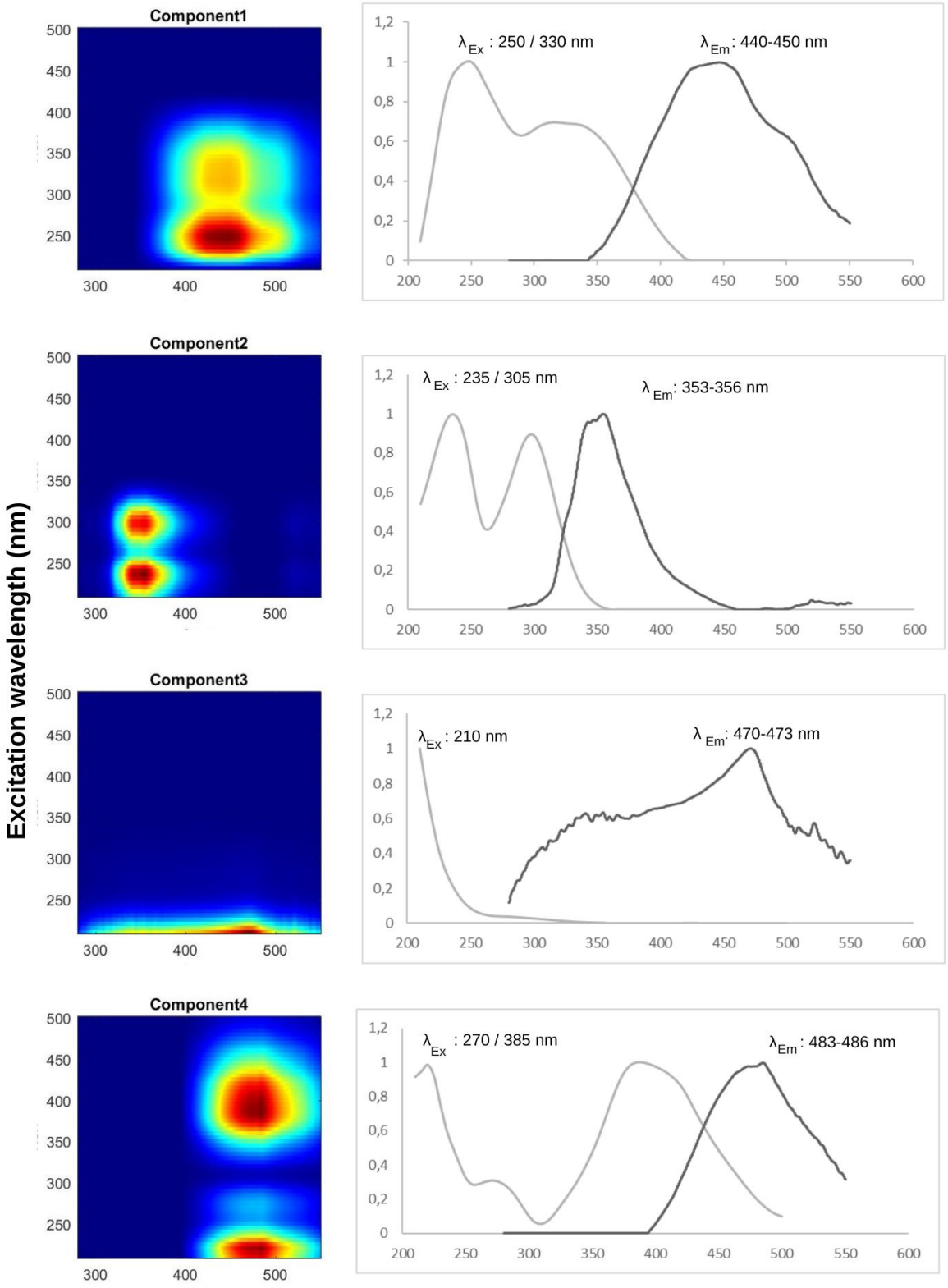

Figure 6: Spectral characteristics of the 4 fluorophores approved by the PARAFAC model for samples from 4 sites (VKP, Ouegoa, Dumbéa, South of Nouméa). In the left column, the plot contours, and the right column the excitation (grey) and emission (black) spectra.

Table 5: Maximum excitation and emission of the 4 fluorophores approved by the PARAFAC model and identification of the compounds by comparison with the literature

4 sites (VKP, Ouegoa, Dumbéa, South of Nouméa)				Previous study			
Component	Ex (nm)	Em (nm)	Type	Comp.	Ex (nm)	Em (nm)	References
C1	250	440-450	Humic-like	A	230-260	400-480	Coble (1996)
	330		Humic-like	M region	312	420/480	(Shank et al., 2010)
C2	235/305	353-356	Tryptophane-like	T1	220-235	334-360	Coble (1996)
C3	210	470-473	Fulvic acid	Region III	200-250	380-550	(Chen et al., 2003)
C4	270/385	483-486	Humic-like terrestrial		370-390	460-480	(Baker, 2001 & 2002)

Four fluorophores were identified in the surface sediment pore waters from the whole sampling sites. By comparing the excitation and emission wavelengths of each of them with the literature, we identified C1 as a *marine* humic-*like* fluorophore, C2 as a tryptophan-*like* fluorophore, C3 as a fulvic acid and finally C4 seems to be more complex with both a humic-*like* and *other* peak, which is typical of terrestrial origin. Although the compounds identified in the 4 sites were similar, their pseudo-concentration differed (Fig. 7, Fig.8 and Table A4 Appendix).

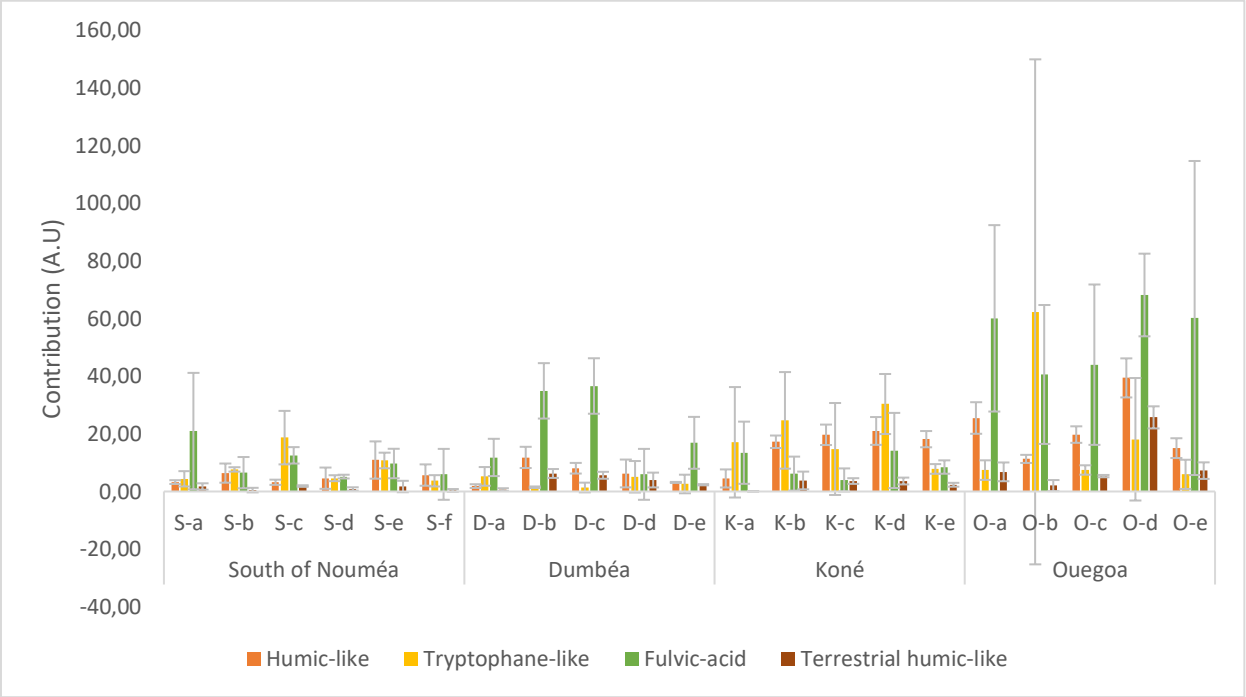

Figure 7: Graph showing the contribution (pseudo-concentration) of the different fluorophores detected by the PARAFAC analysis at the four sampling sites of the ECOMINE campaign. The colour bar represent the mean contribution at each station and the greys line represent the standard deviation. The fluorophore C1 (Humic-like) is represented in orange, the tryptophan-like (C2) in yellow, the Fulvic-acid in green (C3) and the terrestrial humic-like (C4) in brown.

The contribution of fluorophores in FDOM was very heterogeneous at the global level (Fig.7) but also within each site. The most represented fluorophores in order were Fulvic-acid (more abundant in DU and OA, two non-mine-impacted sites) and tryptophan-like, followed by humic-like and finally humic-like of terrestrial origin, which were present mainly in the OA and DU stations (Fig. 8).

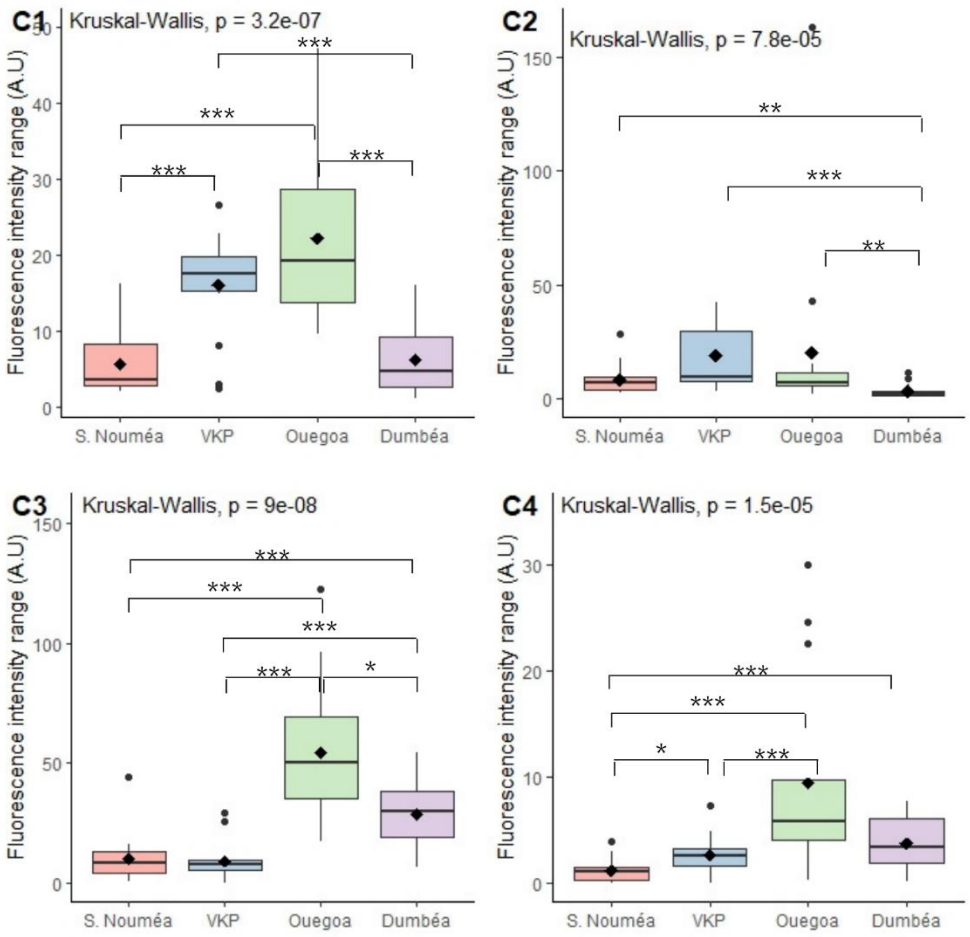

Figure 8: Box plots of DOM fluorescence of four components validated by PARAFAC (C1–C4) in four sites. The mean value is indicated by a black diamond and the median by a black bar. The fluorophore C1 (Humic-like), the tryptophan-like (C2), the Fulvic-acid (C3) and the terrestrial humic-like (C4). Note that the ordinate axes are not the same between fluorophores.

At SN, the mean pseudo-concentration of the Tryptophan-like compound (C2) varied for all stations from 3.69 ± 1.96 (A.U) to 18.67 ± 9.67 (A.U), the Fulvic-acid (C3) ranged from 5.16 ± 0.65 (A.U) to 20.96 ± 20.18 (A.U) (Table A4; Appendix). Humic-like (C1) varied from 3.19 ± 0.90 (A.U) to 10.89 ± 6.47(A.U); humic-like compound of terrestrial origin (C4) varied from 0.38 ± 0.46 (A.U) to 1.88 ± 0.28 (A.U).

The DU site had a much higher mean pseudo-concentration n of Fulvic acid varying from 5.94 ± 8.83 (A.U) to 36.57± 9.62 (A.U). Humic-like and Tryptophan-like were respectively between 1.86 ± 0.65 (A.U) - 11.8 ± 3.68 (A.U) and 1.38 ± 1.69 (A.U) - 3.25. The contribution of humic-like from land was more represented than in the sites of VKP and SN varying from 0.63 ± 0.49 (A.U) to 6.24 ± 1.55 (A.U).

The VKP site had the lowest pseudo-concentration of humic-like terrestrial (C4) (0.04 ± 0.07 (A.U) with a maximum of 3.81 ± 3.07 (A.U). The acid-Fulvic (C3) was weakly represented [3.99 ± 4.00 (A.U) - 14.21 ± 13.03 (A.U)] than in the other sites. The contribution of Tryptophan-like (C2) was important in VKP, increasing from 7.81 ± 1.68 (A.U) to 30.32 ± 10.42 (A.U). The pseudo-concentration of humic-like (C1) ranged from 4.51 ± 3.14 (A.U) and 20.98 ± 4.82 (A.U).

Finally, the OA site had the highest mean station pseudo-concentrations with 39.38 ± 6.77 (A.U) for humic-like, 62.28 ± 87.55 (A.U) for tryptophan-like, 68.13 ± 14.33 (A.U) for acid-Fulvic and 25.69 ± 3.84 (A.U) for humic-like.

Statistically, the C1 fluorophore contributions were not significantly different between the OA and VKP sites, as well as between the DU and SN sites (Fig. 8). The pseudo contributions of the C2 compound at DU site appear to be significantly different from the three other sites, representing a very low tryptophan-like contribution at DU. Concerning the Humic-like-terrestrial compound C4, the contributions were highest and not significantly different between the OA and DU sites. The same trend was observed for Fulvic acid (C3). However, a significant difference was shown between the two sites, OA being more highly concentrated in Fulvic acid than DU.

The fluorescence indices, HIX and BIX, are calculated to confirm the origin of either terrigenous or microbial loops in the surface sediment pore waters. The average indices for each station are grouped in Table A.3 in Appendix. The HIX mean values were generally higher than the BIX values for all sites (Fig.9). However, the variability between station for each indicator and for each site was high (boxplot size) indicating a higher station effect than a site effect.

From a statistical perspective on the HIX index, intra-site differences were observed for the DU site ($p < 0.05$), with a significant difference between station A and B (p-value < 0.01; Wilcoxon) and between B and E (p-value < 0.05; Wilcoxon) (Appendix A5) and for SN site ($p = 0.05$). Due to the high variability within sites, no significant differences were found between sites (inter-site) (p-value = 0,17 ; Kruskal-Wallis) (Fig.9.B). For the BIX indices, no intra-site differences were observed (Appendix A5). With the non-parametric one-way ANOVA test, the Kruskal-Wallis rank sum test, at least one significant difference was observed between the 4 sites, however the post-hoc non-parametric Wilcoxon rank sum test does not has the same power, so no differences could be determined (Fig.9.A).

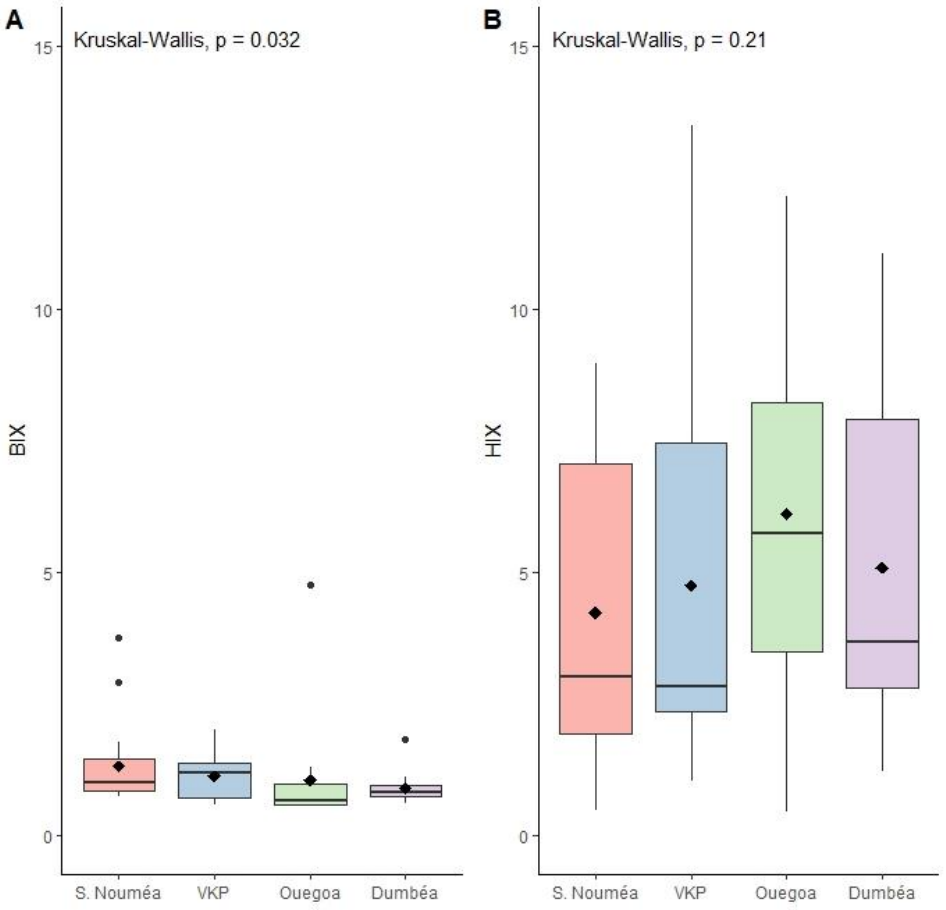

Figure 9: Box plot illustrating inter-site variability about the HIX, and BIX indexes calculated on the 4 sites during the ECOMINE Campaign (March-April 2022). A: BIX, B: HIX.

In order to confirm the identification of the four fluorophores, a correlation analysis between the physico-chemical and optical parameters and the fluorescence intensity was carried out. The choice of variables was made according to a Spearman correlation matrix (Appendix A4), when some variables were strongly correlated with each other, only one of them was retained in order not to bias the PCA.

The principal component analysis carried out for all the sites allows 46% of the variance observed to be represented (Fig. 9), (31% for axis 1 and 15% for axis 2).

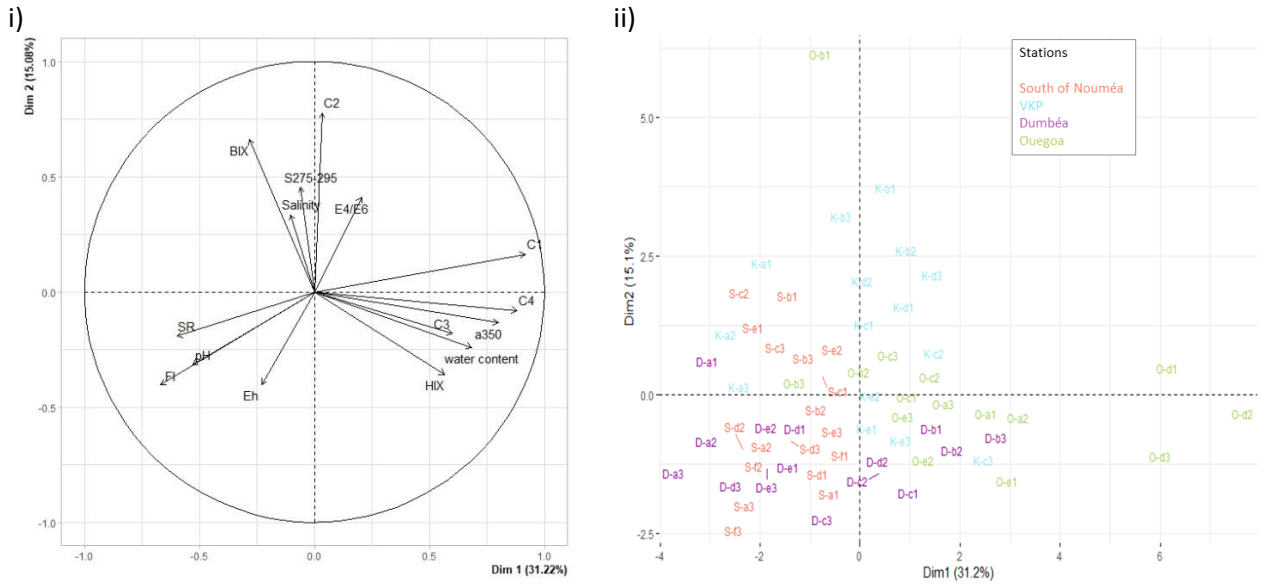

Figure 10: Principal component analysis (PCA) based on Spearman correlation matrices between CDOM/FDOM and physico-chemical parameters. All the stations were integrated in the PCA (n=63)

On the correlation circle (Fig. 10.i), on the right of axis 1 are placed the water content and the a_{350} coefficient (proxy of terrigenous input). This coefficient was highly correlated to the two other absorbance coefficients a_{442} and a_{254} (Appendix A4): the more the coordinates of the stations are positive on this axis, the more the samples were characterised by their terrigenous origin of the DOM and water content. This characteristic concerning the terrigenous origin is supported by a positive positioning of HIX (humification indicator) and the nature of the fluorophore C4, which was identified as strongly terrestrial. The S_R ratio, pH and fluorescence index are negatively set on axis 1. Axis 2 positively places the fluorophore C2 (Tryptophan-like) as well as the BIX index (biological activity indicator), salinity, the E4/E6 index and the spectral slope index $S_{275-295}$. This slope was highly correlated to $S_{350-400}$ and E2/E3 (Appendix A4). The more positive the coordinates of the stations on this axis, the more the samples were characterised by their biological activity. Axis 2 opposes the molecular weight indicator E4/E6 and the Eh (negatively located on the axis); the lower the Eh, the higher the E4/E6, suggesting high molecular weight molecules.

Samples from OA and DU are more influenced by dimension 1 (Fig. 10.ii). On the contrary, the DU samples are more represented on the left side, the variables associated with pH, S_R (photodegradation indicator) as well as the fluorescence index have a more important influence in DU for the distribution of the samples. All DU samples are located on the negative side of dimension 2, showing a very low biological activity.

Samples from VKP and some SN stations are more represented by dimension 2. The VKP stations show a greater contribution from the C2 compound (Tryptophan-like) and biological activity in the whole, than those of the SN site, which are more influenced by the Eh and the fluorescence index.

4 DISCUSSION

4.1 CHARACTERISTICS OF CDOM IN SEDIMENT PORE WATERS

Sites under the influence of ultramafic massifs (strong to moderate) seem to have low molecular weight dissolved organic matter in their sediments (SR>1: VKP, DU, SN) (Hansen et al., 2016). The two most impacted mining sites (VKP and SN) showed very low concentrations of DOM of both terrestrial and biological origin, these two sites are almost entirely located in ultramafic massif, respectively the Koniambo massif (Perrier *et al*., 2006) and the grand massif of south of New-Caledonia (Fernandez et al., 2017).

On the other hand, the OA site was characterized by the highest concentration of organic matter in the coastal sediments. This DOM seems to be of high molecular weight and could be explained by a strong contribution of OM from terrigenous inputs. In their study Pages & Gadel, (1990) found that mangrove pore waters appeared to be of higher molecular weight than pore waters from river sediments. All this observation does not seem to hold for the VKP site, which is also heavily bordered by mangroves.

Our spectral slope results [0.005-0.015] and S_R [0.94-1.77] value (related to the molecular weight as well as the photodegradation process) are low compared to literature. Studies have shown that ocean waters have a $S_{275-295}$ value between 0.020-0.030 nm and a Sr value between 1.6-3.4 (Hansen *et al*., 2016). Moreover, coastal waters have a $S_{275-295}$ value between 0.010-0.020 nm and between 0.014-0.018 nm for wetlands, which are also characterized by a Sr value between 0.76-1 (Hansen *et al*., 2016). The spectral slope values in the sediments are lower, approaching wetland (Clark et al., 2014). As the lower the spectral slope value (S) the higher the molecular weight (Hansen et al., 2016), sediments in our study shows that OA site was defined by molecules of higher molecular weight than those present in the other sampled sites. In contrast the spectral slope values were the highest for the VKP site, which suggests that the organic matter present in this estuary is characterized by very low molecular weight compared to the other sites.

Furthermore, the aromaticity and size of VKP humic substances were the smallest in the dataset (high E2/E3 value). The matter found at VKP could be explained by greater biological activity than in other sampled site (second highest mean BIX value after SN site). Studies have shown that molecules from microbial activity, such as exudation and release of cell contents, which are part of the normal cell growth cycle, can be the source of small molecules (Mayer *et al*.,1999).

On the other hand, the humic substance sizes were the highest for the DU stations (E2/E3 almost always around 1.2 for all DU stations). The site SN was more variable with stations that had a high E2/E3 (3.62) similar to those in VKP and stations that had a very low E2/E3 (1.29) as at DU (Appendix; Table A2). The variability in terms of molecule size at SN could be explained by the characteristics of the site, which is both urbanised like DU and potentially subject to anthropogenic inputs but also close to mining sites and on the same soil type such as at VKP (Losfeld *et al*., 2015).

4.2 SOURCES OF DOM IN SEDIMENT PORE WATERS

C1 was found in abundance at the OA and VKP sites as well as for the stations (B, C, D) of DU which are strongly surrounded by mangroves. This fluorophore is characterised by two peaks A and M. Shank et al. (2010) reported that mangrove leached material had a majority of humic A fluorophores. They also show the presence of peak M from autochthonous origin and typical of mangroves. Tannins from senescent mangrove leaves could be the source of M-type humic acid in tropical and subtropical regions with prolonged light exposure (Maie et al., 2008). In view of the agreement of the results

obtained in our study and those obtained by Maie et al. (2008) and Shank et al. (2010) both on mangroves, it would seem that our C1 compound might indicate mangrove origin. These two peaks were already found in the water column at DU in New-Caledonia in a study conducted by Martias, (2018). However its humic-like compound was more correlated with other compounds of biological origin (tryptophan-like and tyrosin-like compounds), suggesting in this case that the compound originated from marine plankton production.

Compound C2, identified as a tryptophan-like, had a rather homogeneous distribution along the sites (OA, SN and DU) with a higher concentration at VKP. This compound of autochthonous origin could be derived from heterotrophic bacteria (Coble, 1996). However Zhao et al. (2017) reported that tryptophan-like compounds are likely to originate from polluted water discharge rather than biological activity. Given the correlations between the tryptophan-like compound and indicators of biological activity (BIX, E2/E3, as well as S-spectral slopes), biological origin seems to be considered in priority in our study. Further research to characterise the bacterial activity would be essential to clearly identify the biological sources of these compounds. Sediment samples were collected during the ECOMINE campaign to analyse the microbial compartment using the eDNA metabarcoding tool. These analyses should shed light on the composition of the communities in the different sediments.

Compounds C3 and C4, respectively fulvic acid and terrestrial humic-like, showed the same tendency towards their contributions (high for the OA and DU, and lower for the VKP and SN). Hood et al. (2003) showed that the high presence of fulvic acid was often linked to an allochthonous origin of dissolved carbon. This difference between the sites would be explained by more important fluvial inputs at OA and DU. Indeed, the Diahot is the largest river in New Caledonia and the Dumbéa watershed is the source of large freshwater inflows (Bird et al., 1984 ; Fernandez et al., 2017). On the other hand, the very low concentration of fulvic acid in the VKP and SN sites may suggest a higher biological activity in these two sites. Similarly, McKnight *et al.* (1994) demonstrated that autochthonous MOD from bacterial biomass was characterised by low fulvic acid concentrations.

In fact, both fulvic and humic acids are derived from humic matter (from the plant and animals degradation) with a similar structure but differ in their water solubility, functional group composition and molecular weight (Kim et al.,1990). Fulvic acids are soluble in water at any pH, whereas humic acids are soluble only under alkaline conditions (pH > 2) (Gaffney et al.,1996). In our study, the pH conditions were always above 7, so both acids were in their soluble form. The terrestrial origin of these two compounds seems to be linked in our study with the important input of river water potentially highly loaded in humic matter.

Fluorescence results in our study are consistent with results published recently in a study conducted in the coastal region of the East China Sea showing that in pore waters collected in forty-two sites the presence of three protein-like compounds and two Humic-like compounds (Li *et al.*, 2020). Their origins were both autochthonous (microbial production) and allochthonous. Although in our study, fewer autochthonous molecules were identified. Otero et al. (2007) argue that in estuarine, the fluorescence properties may reflect the contribution of complex origin of organic materials. Indeed, we found two compounds that seem to come from fluvial inputs (Humic-like and Fulvic-acid), as well as autochthonous compounds of both biological origin (Tryptophan-like) and from mangroves (Humic-like).

4.3 FACTORS AFFECTING THE VARIABILITY OF THE DOM COMPARTMENT WITHIN A SINGLE GLOBAL GEOGRAPHICAL AREA (NEW CALEDONIA)

The variability of the DOM characteristics within the study sites could be explained by the large differences and complexity of the sampled environments. Although the characteristics of the DOM

found in each site are a unique set of molecules, similarities between sites were found. Three main factors influencing DOM were highlighted (soil geology, mangroves, and watershed size) (Table 6).

Other studies have identified multiple factors influencing the quality or quantity of DOM in various ecosystems. Similarly, Li et al. (2020) have revealed the complex sources of humic-like substances from both microbial and terrestrial activities in the pore water sediment of China. Yamashita et al., (2010) have highlighted the effect of soil geology and hydrodynamics on the DOM present in the water column of tropical rivers in Venezuela. On other hand Martias et al. (2018), have highlighted the effect of coral and ocean activity on DOM in the New Caledonian lagoon.

Table 6: Main factors that may influence the DOM characteristics, based on the result of characterisation of DOM from optical analyses (CDOM and FDOM). The factor link to ultramafic soil is in red, biological activity in blue, impact of mangrove in green and impact of the fluvial input in brown.

South of Nouméa	VKP	Ouegoa	Dumbéa
Low amount of DOM (a350, a254)	Low amount of DOM (a_{350}, a_{254}) Lowest molecular weight (S)	High amount of DOM (a350, a254) Terrestrial molecules with hight molecular weight (SR)	High amount of DOM (a350, a254) Highest molecular weight (S)
More or less aromatic molecules between the sites (E2/E3)	Small and aromatic molecule (E2/E3)		Large aromatic molecule (E2/E3)
	A lot of C1 (humic-like-mangrove)	A lot of C1 (humic-like-mangrove)	Few Tryptophane-like (C2)
	Lots of C2 (Tryptophane-like)	Lots of fulvic acid (C3) and terrestrial-humic-like (C4)	Lots of fulvic acid (C3) and terrestrial-humic-like (C4)
Few fulvic acid (C3)	Few fulvic acid (C3)		

4.3.1 Effect of mangroves

The VKP and OA sites are characterized by the presence of dense mangroves. This vegetation, especially senescent mangrove leaves and litter, could explain the presence of the humic-like-mangrove fluorophore (C1) found in the sediment of these sites. Indeed, studies have shown that mangrove litter represents an important organic carbon reservoir (Alongi, 1997). In their study, Marchand et al. (2011) have shown that mangroves in southern New Caledonia (Conception Bay) are supplemented with organic carbon. The large portion of organic carbon coming from mangroves could explain the high contribution of mangrove humic acid at the VKP and OA sites and their very low representation at the other two sites, where mangrove are patchy. Moreover, the continuous input of mangrove debris is responsible for the variation of physico-chemical conditions between stations, constituting unique conditions at different points within the same site (Marchand et al., 2012). This result is in line with the intra-site variability we found for C1 contributions at the VKP and OA sites.

4.3.2 Possible impact of catchment size and river input

The OA and DU sites share common characteristics in the DOM compartment. The large amount of CDOM, the high molecular weight of DOM, the high contribution of acid-fulvic and humic-like

terrestrial fluorophores are all parameters that seem to point to an impact of riverine inputs. Moreover, these two sites are those of the study with the largest catchment areas and therefore the highest river flow rates and material inputs (Bird *et al.*, 1984; Alric, 2009; Fernandez et al., 2017). Our results are supported by those of Yamashita et al. (2010) who found that in their study sites during the wet season, when river flows are highest, the effluent was heavily composed of DOM of terrestrial origin. Although the size of the catchment area has an impact on the characteristics of the DOM, the residence time of the water in the estuary could also be an influencing factor. Indeed, Battin et al. (2008) showed in the water column in an estuary that the characteristics of dissolved organic matter were strongly related to the residence time of river water.

4.3.3 Possible impact of the geological composition of the soil (ultramafic)

The sites under ultramafic influence seem to share the same characteristics, low amount of MOD and a high biological activity as mentioned above. The low pseudo-concentrations of some FDOM compounds in this environment could be explained by a quenching phenomenon. This is a process that inhibits fluorescence, a quencher (usually metallic) collides with the excited fluorophore, causing the fluorophore to de-excite. This type of static quenching is the major one in natural FDOMs (Wang et al., 2017). Indeed, metal produced in sediment under ultramafic influence could have altered the fluorescence properties of DOM. Therefore, it would explain why terrestrial molecules with high molecular weight was less detected in our study at VKP, SN and DU. Indeed In the same way, Mayer et al. (1999) have highlighted in their study that terrestrial inputs could cause difficulties in recording protein-like molecules. Data from analyses of metal concentrations in pore water will help us to estimate the effect of a quenching process. An experiment could then be carried out using our samples to test on this process the effect of the main metals naturally present (Ni and Cu) in the sampling sites (Bessard, 2019).

In addition to the impact of quenching, biological activity may also be one of the causes of a part the low amount of CDOM observed in the samples from the VKP and SN sites. In fact, the low a_{350} values found at the two sites under ultramafic soil influences suggest an autochthonous DOM activity, as found in the Guayana Shield lagoon highly impacted by gold mining (Yamashita et al., 2010). Furthermore, Martias et al. (2018) have also already demonstrated the removal of CDOM by biological processes in the lagoon of New Caledonia, which has a high level of phytoplankton activity compared to other tropical lagoons such as Reunion Island (Tedetti et al., 2011). At the SN and VKP sites, the indicators of molecular weight (S) and aromaticity (E2/E3) as well as the high presence of tryptophan at VKP and the low representation of fulvic acid are parameters that seem to represent a high biological activity at these two sites (table 6). This assumption concerning biological activity might be confirmed. The presence of certain metals such as iron could promote biological activity (Tagliabue et al., 2017).

5 CONCLUSION AND PERSPECTIVES

By characterizing the MOD of sediment pore water under different geological influences, four fluorophores have been characterized with EEMs-PARAFAC. It is found that the pore water DOM is composed of both autochthonous (C1, C2) and allochthonous (C3, C4) material. A strong site effect has been identified, which can be explained by three main factors. One of the factors is the presence of mangrove, which influences the occurrence of humic-like-mangrove compounds (C1), which are strongly represented in the VKP and OA sites. Secondly, the size of the catchment areas and the hydrodynamic inputs cause a high abundance of terrestrial humic-like compounds and acid-fulvic compounds, especially for the DU and OA sites. Finally, it would appear that the geology of the soils, particularly the ultramafic soils, as well as the presence of mining activity would have an impact on the

DOM characteristics, as the VKP and SN sites, which are a low CDOM content and highest biological activity.

However, some of the variability in the study is strongly associated with variations within sites. Our results indicate high variable physico-chemical conditions at station level in several sites. Burdige (2001) has shown that sediment redox conditions, as well as remineralisation, impact MOD concentrations. Gan et al. (2020) demonstrated that sulphate reduction (low redox conditions) stimulates OM fluxes from the particulate to the dissolved compartment and thus lead to DOC accumulation in pore waters. In very reduced conditions, they also found that microbial activity is less efficient (production of dissolved organic carbon and hydrolysis), to compensate this difficulty the microorganisms use humic-like. Moreover, low Eh values found in several stations could modify the bioavailability of certain elements such as metallic derivatives (iron, manganese, copper, chromium, etc.) but also nitrogenous and phosphorus compounds in the sediment (Cabridenc, 1991 ; Luek et al., 2017). Considering this knowledge, the data set should be analysed at the intra-site level to estimate the effects of the different environmental factors influencing the concentrations and characteristics of the DOM. Numerous ongoing analyses within the framework of the Ecomine project should advance our knowledge of the behaviour of DOM in ecosystems subjected to ultramafic inputs.

6 REFERENCES

Abaker, M. G. (2016). *Suivi de maturation de composts mixtes par spectrométrie d ' absorption et de fluorescence UV-Vis*.

Alongi, D. . (1997). *Coastal ecosystem processes* (CRC Press). New-York.

Alric, R. (2009). *Recueil des débits caractéristiques de la Nouvelle-Calédonie. (Nouméa : Direction des Affaires Veterinaires Alimentaires et Rurales (DAVAR)).*

Ambatsian, P., Fernex, F., Bernat, M., Parron, C., & Lecolle, J. (1997). High metal inputs to closed seas: The New Caledonian lagoon. *Journal of Geochemical Exploration*, *59*(1), 59–74. https://doi.org/10.1016/S0375-6742(96)00020-9

Audet, M.-A. (2009). *en Sciences de la Terre - Pétrologie et Minéralogie Le massif du Koniambo , Nouvelle-Calédonie Formation et obduction d ' un complexe ophiolitique du type SSZ . Enrichissement en nickel , cobalt et scandium dans les profils résiduels*.

Baker, A. (2001). Fluorescence excitation - Emission matrix characterization of some sewage-impacted rivers. *Environmental Science and Technology*, *35*(5), 948–953. https://doi.org/10.1021/es000177t

Baker, A. (2002). Fluorescence excitation-emission matrix characterization of river waters impacted by a tissue mill effluent. *Environmental Science and Technology*, *36*(7), 1377–1382. https://doi.org/10.1021/es0101328

Battin, T. J., Kaplan, L. A., Findlay, S., Hopkinson, C. S., Marti, E., Packman, A. I., … Sabater, F. (2008). Biophysical controls on organic carbon fluxes in fluvial networks. *Nature Geoscience*, *1*(2), 95–100. https://doi.org/10.1038/ngeo101

Benavides, M., Martias, C., Elifantz, H., Berman-Frank, I., Dupouy, C., & Bonnet, S. (2018). Dissolved organic matter influences N2 fixation in the New Caledonian lagoon (western tropical South Pacific). *Frontiers in Marine Science*, *5*(MAR), 1–11. https://doi.org/10.3389/fmars.2018.00089

Bessard, M. (2019). *Complexation des ETM par la MOD Analyse par extinction de fluorescence sur un continiuum rivière-mangrove-lagon dans la province Nord de la Nouvelle-Calédonie*.

Bird, E. C. ., Dubois, J. ., & Iltis, J. . (1984). The Impact of Opencast Mining on the Rivers and Coasts of New Caledonia. Retrieved June 1, 2022, from The United Nation University : Shibuya, Japan website: http://archive.unu.edu/unupress/%0Aunupbooks/80505e/80505E00.htm

Black, M. (1977). *Regional high-pressure metamorphism in new caledonia: Phase equilibria in the ouégoa district*. *43*, 89–107.

Bonvallot, J., Gay, Jean-Christophe Habert, E., & IRD, C. (2013). *Atlas de la Nouvelle-Calédonie*.

Bricaud, A., Morel, A., & Prieur, L. (1981). Absorption by dissolved organic matter of the sea (yellow substance) in the UV and visible domains. *Limnology and Oceanography*, *26*(1), 43–53. https://doi.org/10.4319/lo.1981.26.1.0043

Bro, R. (1997). PARAFAC. Tutorial and applications. *Chemometrics and Intelligent Laboratory Systems*, *38*(2), 149–171. https://doi.org/10.1016/S0169-7439(97)00032-4

Burdige, D. J. (2001). Dissolved organic matter in Chesapeake Bay sediment pore waters. *Organic Geochemistry*, *32*(4), 487–505. https://doi.org/10.1016/S0146-6380(00)00191-1

Burdige, D. J., Kline, S. W., & Chen, W. (2004). Fluorescent dissolved organic matter in marine sediment pore waters. *Marine Chemistry*, *89*(1–4), 289–311. https://doi.org/10.1016/j.marchem.2004.02.015

Chen, M., & Hur, J. (2015). Pre-treatments, characteristics, and biogeochemical dynamics of dissolved organic matter in sediments: A review. *Water Research*, *79*, 10–25. https://doi.org/10.1016/j.watres.2015.04.018

Chen, W., Westerhoff, P., Leenheer, J. A., & Bookh, K. (2003). Fluorescence Excitation-Emission Matrix Regional Integration to Quantify Spectra for Dissolved Organic Matter. *Environmental Sciences & Technology*. https://doi.org/https://doi.org/10.1021/es034354c

Clark, C. D., Aiona, P., Keller, J. K., & De Bruyn, W. J. (2014). Optical characterization and distribution of chromophoric dissolved organic matter (CDOM) in soil porewater from a salt marsh ecosystem. *Marine Ecology Progress Series*, *516*, 71–83. https://doi.org/10.3354/meps10833

Coble, P. G. (1996). Characterization of marine and terrestrial DOM in seawater using excitation-emission matrix spectroscopy. *Marine Chemistry*, *51*(4), 325–346. https://doi.org/10.1016/0304-4203(95)00062-3

Coble, P. G. (2007). Marine optical biogeochemistry: The chemistry of ocean color. *Chemical Reviews*, *107*(2), 402–418. https://doi.org/10.1021/cr050350+

Desclaux, T., Lemonnier, H., Genthon, P., Soulard, B., & Le Gendre, R. (2018). Suitability of a lumped rainfall–runoff model for flashy tropical watersheds in New Caledonia. *Hydrological Sciences Journal*, *63*(11), 1689–1706. https://doi.org/10.1080/02626667.2018.1523613

Destoumieux-Garzón, D., Mavingui, P., Boetsch, G., Boissier, J., Darriet, F., Duboz, P., … Voituron, Y. (2018). The one health concept: 10 years old and a long road ahead. *Frontiers in Veterinary Science*, *5*(FEB), 1–13. https://doi.org/10.3389/fvets.2018.00014

Dupouy, C., Röttgers, R., Tedetti, M., Frouin, R., Lantoine, F., Rodier, M., … Goutx, M. (2020). Impact of Contrasted Weather Conditions on CDOM Absorption/Fluorescence and Biogeochemistry in the Eastern Lagoon of New Caledonia. *Frontiers in Earth Science*, *8*(March). https://doi.org/10.3389/feart.2020.00054

Faure, V., Pinazo, C., Torréton, J. P., & Jacquet, S. (2010). Modelling the spatial and temporal variability of the SW lagoon of New Caledonia I: A new biogeochemical model based on microbial loop recycling. *Marine Pollution Bulletin*, *61*(7–12), 465–479.

https://doi.org/10.1016/j.marpolbul.2010.06.041

Fernandez, J. M., Meunier, J. D., Ouillon, S., Moreton, B., Douillet, P., & Grauby, O. (2017). Dynamics of suspended sediments during a dry season and their consequences on metal transportation in a Coral reef lagoon impacted by mining activities, New Caledonia. *Water (Switzerland)*, *9*(5). https://doi.org/10.3390/w9050338

Fichez, R., Chifflet, S., Douillet, P., Gérard, P., Gutierrez, F., Jouon, A., … Grenz, C. (2010). Biogeochemical typology and temporal variability of lagoon waters in a coral reef ecosystem subject to terrigeneous and anthropogenic inputs (New Caledonia). *Marine Pollution Bulletin*, *61*(7–12), 309–322. https://doi.org/10.1016/j.marpolbul.2010.06.021

Folcher, N., Sevin, B., Quesnel, F., Lignier, V., Allenbach, M., Maurizot, P., & Cluzel, D. (2015). Neogene terrestrial sediments: A record of the post-obduction history of New Caledonia. *Australian Journal of Earth Sciences*, *62*(4), 479–492. https://doi.org/10.1080/08120099.2015.1049207

Gaffney, J. S., Marley, N. A., & Clark, S. B. (1996). Humic and Fulvic Acids and Organic Colloidal Materials in the Environment. *ACS Symposium Series*, *651*. https://doi.org/10.1021/bk-1996-0651.ch001

Gan, S., Schmidt, F., Heuer, V. B., Goldhammer, T., Witt, M., & Hinrichs, K. U. (2020). Impacts of redox conditions on dissolved organic matter (DOM) quality in marine sediments off the River Rhône, Western Mediterranean Sea. *Geochimica et Cosmochimica Acta*, *276*, 151–169. https://doi.org/10.1016/j.gca.2020.02.001

Gauthier, T. D., Shane, E. C., Guerin, W. F., Seitz, W. R., & Grant, C. L. (1986). Fluorescence quenching method for determining equilibrium constants for polycyclic aromatic hydrocarbons binding to dissolved humic materials. *Environ. Sci. Technol.*

Hansen, A. M., Kraus, T. E. C., Pellerin, B. A., Fleck, J. A., Downing, B. D., & Bergamaschi, B. A. (2016). Optical properties of dissolved organic matter (DOM): Effects of biological and photolytic degradation. *Limnology and Oceanography*, *61*(3), 1015–1032. https://doi.org/10.1002/lno.10270

Hautala, K., Peuravuori, J., & Pihlaja, K. (2000). Measurement of aquatic humus content by spectroscopic analyses. *Water Research*, *34*(1), 246–258. https://doi.org/10.1016/S0043-1354(99)00137-2

Helms, J., Stubbins, A., Ritchie, J. D., Minor, E. C., Kieber, D. J., & Mopper, K. (2008). Absorption spectral slopes and slope ratios as indicators of molecular weight, source, and photobleaching of chromophoric dissolved organic matter (Limnology and Oceanography 53 955-969). *Limnology and Oceanography*, *54*(3), 1023. https://doi.org/10.4319/lo.2009.54.3.1023

Hood, E., McKnight, D. M., & Williams, M. W. (2003). Sources and chemical character of dissolved organic carbon across an alpine/subalpine ecotone, Green Lakes Valley, Colorado Front Range, United States. *Water Resources Research*, *39*(7), 1–12. https://doi.org/10.1029/2002WR001738

Kim, J. I., Buckau, G., Li, G. H., Duschner, H., & Psarros, N. (1990). Characterization of humic and fulvic acids from Gorleben groundwater. *Fresenius' Journal of Analytical Chemistry*, *338*(3), 245–252. https://doi.org/10.1007/BF00323017

Laganier, R. (1994). *Contribution à l'étude des processus d'érosion et des risques naturels dans les iles du sud-ouest Pacific (Nouvelle-Calédonie et iles Salomon)*. Lille.

Lalau, N., Soulard, B., & Le Gendre, R. (2019). *Atlas 2011-2017 des apports hydriques à l ' échelle du territoire calédonien Projet Présence*.

Li, M., Xie, W., Li, P., Yin, K., & Zhang, C. (2020). Establishing a terrestrial proxy based on fluorescent dissolved organic matter from sediment pore waters in the East China Sea. *Water Research*, *182*, 116005. https://doi.org/10.1016/j.watres.2020.116005

Lillie, A. R. (1970). The structural geology of lawsonite and glaucophane schists of the ouégoa district, new caledonia. *New Zealand Journal of Geology and Geophysics*, *13*(1), 72–116. https://doi.org/10.1080/00288306.1970.10428207

Losfeld, G., L'Huillier, L., Fogliani, B., Jaffré, T., & Grison, C. (2015). Mining in New Caledonia: environmental stakes and restoration opportunities. *Environmental Science and Pollution Research*, *22*(8), 5592–5607. https://doi.org/10.1007/s11356-014-3358-x

Luek, J. L., Thompson, K. E., Larsen, R. K., Heyes, A., & Gonsior, M. (2017). Sulfate Reduction in Sediments Produces High Levels of Chromophoric Dissolved Organic Matter. *Scientific Reports*, *7*(1), 1–8. https://doi.org/10.1038/s41598-017-09223-z

Maie, N., Pisani, O., & Jaffé, R. (2008). Mangrove tannins in aquatic ecosystems: Their fate and possible influence on dissolved organic carbon and nitrogen cycling. *Limnology and Oceanography*, *53*(1), 160–171. https://doi.org/10.4319/lo.2008.53.1.0160

Marchand, C., Allenbach, M., & Lallier-Vergès, E. (2011). Relationships between heavy metals distribution and organic matter cycling in mangrove sediments (Conception Bay, New Caledonia). *Geoderma*, *160*(3–4), 444–456. https://doi.org/10.1016/j.geoderma.2010.10.015

Marchand, C., Fernandez, J. M., Moreton, B., Landi, L., Lallier-Vergès, E., & Baltzer, F. (2012). The partitioning of transitional metals (Fe, Mn, Ni, Cr) in mangrove sediments downstream of a ferralitized ultramafic watershed (New Caledonia). *Chemical Geology*, *300–301*, 70–80. https://doi.org/10.1016/j.chemgeo.2012.01.018

Martias, C. (2018). *Dynamique de la matière organique dissoute colorée et fluorescente en zone logonaire tropicale dans le Pacifique Sud (Nouvelle Calédonie) : influences climatique et antropogéniques*. Marseille.

Martias, C., Tedetti, M., Lantoine, F., Jamet, L., & Dupouy, C. (2018). Characterization and sources of colored dissolved organic matter in a coral reef ecosystem subject to ultramafic erosion pressure (New Caledonia, Southwest Pacific). *Science of the Total Environment*, *616–617*, 438–452. https://doi.org/10.1016/j.scitotenv.2017.10.261

Massicotte, P., & Markager, S. (2016). Using a Gaussian decomposition approach to model absorption spectra of chromophoric dissolved organic matter. *Marine Chemistry*, *180*, 24–32. Retrieved from http://linkinghub.elsevier.com/retrieve/pii/S0304420316300081

Mayer, L. M., Schick, L. L., & Loder, T. C. (1999). Dissolved protein fluorescence in two maine estuaries. *Marine Chemistry*, *64*(3), 171–179. https://doi.org/10.1016/S0304-4203(98)00072-3

McKnight, D. M., Andrews, E. D., Spaulding, S. A., & Aiken, G. R. (1994). Aquatic fulvic acids in algal-rich antarctic ponds. *Limnology and Oceanography*, *39*(8), 1972–1979. https://doi.org/10.4319/lo.1994.39.8.1972

McKnight, D. M., Boyer, E. W., Westerhoff, P. K., Doran, P. T., Kulbe, T., & Andersen, D. T. (2001). Spectrofluorometric characterization of dissolved organic matter for indication of precursor organic material and aromaticity. *Limnology and Oceanography*, *46*(1), 38–48. https://doi.org/10.4319/lo.2001.46.1.0038

Mounier, S., Zhao, H., Garnier, C., & Redon, R. (2011). Copper complexing properties of dissolved organic matter: PARAFAC treatment of fluorescence quenching. *Biogeochemistry*, *106*(1), 107–116. https://doi.org/10.1007/s10533-010-9486-6

Nelson, N. B., & Siegel, D. A. (2013). The global distribution and dynamics of chromophoric dissolved organic matter. *Annual Review of Marine Science*, *5*, 447–476. https://doi.org/10.1146/annurev-marine-120710-100751

Oliver, A. A., Spencer, R. G. M., Deas, M. L., & Dahlgren, R. A. (2016). Impact of seasonality and anthropogenic impoundments on dissolved organic matter dynamics in the Klamath River (Oregon/California, USA). *Journal of Geophysical Research: Biogeosciences*, *121*(7), 1946–1958. https://doi.org/10.1002/2016JG003497

Otero, M., Mendonça, A., Válega, M., Santos, E. B. H., Pereira, E., Esteves, V. I., & Duarte, A. (2007). Fluorescence and DOC contents of estuarine pore waters from colonized and non-colonized sediments: Effects of sampling preservation. *Chemosphere*, *67*(2), 211–220. https://doi.org/10.1016/j.chemosphere.2006.10.044

Ouillon, S., Douillet, P., Lefebvre, J. P., Le Gendre, R., Jouon, A., Bonneton, P., … Fichez, R. (2010). Circulation and suspended sediment transport in a coral reef lagoon: The south-west lagoon of New Caledonia. *Marine Pollution Bulletin*, *61*(7–12), 269–296. https://doi.org/10.1016/j.marpolbul.2010.06.023

Paerl, H. W., Pinckney, J. L., Fear, J. M., & Peierls, B. L. (1998). Ecosystem responses to internal and watershed organic matter loading: Consequences for hypoxia in the eutrophying Neuse River Estuary, North Carolina, USA. *Marine Ecology Progress Series*, *166*(May), 17–25. https://doi.org/10.3354/meps166017

Pages, J., & Gadel, F. (1990). Dissolved organic matter and UV absorption in a tropical hyperhaline estuary. *The Science of the Total Environment*, *99*.

Para, J. (2011). *Etude de la Matière Organique Dissoute Chromophorique et du rayonnement solaire (UV-visible) dans les eaux de surface côtières Méditerranéennes et Arctiques*. 1–172.

Parlanti, E., Wörz, K., Geoffroy, L., & Lamotte, M. (2000). Dissolved organic matter fluorescence spectroscopy as a tool to estimate biological activity in a coastal zone submitted to anthropogenic inputs. *Organic Geochemistry*, *31*(12), 1765–1781. https://doi.org/10.1016/S0146-6380(00)00124-8

Payri, C. E., Allain, V., Aucan, J., David, C., David, V., Dutheil, C., … Samadi, S. (2018). New Caledonia. *World Seas: An Environmental Evaluation Volume II: The Indian Ocean to the Pacific*, (March), 593–618. https://doi.org/10.1016/B978-0-08-100853-9.00035-X

Perrier, N., Ambrosi, J. P., Colin, F., & Gilkes, R. J. (2006). Biogeochemistry of a regolith: The New Caledonian koniambo ultramafic massif. *Journal of Geochemical Exploration*, *88*(1-3 SPEC. ISS.), 54–58. https://doi.org/10.1016/j.gexplo.2005.08.015

Roberts, C. M., McClean, C. J., Veron, J. E. N., Hawkins, J. P., Allen, G. R., McAllister, D. E., … Werner, T. B. (2002). Marine biodiversity hotspots and conservation priorities for tropical reefs. *Science*, *295*(5558), 1280–1284. https://doi.org/10.1126/science.1067728

Rocha, J. C., Sargentini, É., Toscano, I. A. S., Rosa, A. H., & Burba, P. (1999). Multi-method Study on Aquatic Humic Substances from the “Rio Negro” - Amazonas State/Brazil. Emphasis on Molecular-Size Classification of their Metal Contents. *Journal of the Brazilian Chemical Society*, *10*(3), 169–175. https://doi.org/10.1590/S0103-50531999000300002

Shank, G. C., Lee, R., Vähätalo, A., Zepp, R. G., & Bartels, E. (2010). Production of chromophoric dissolved organic matter from mangrove leaf litter and floating Sargassum colonies. *Marine Chemistry*, *119*(1–4), 172–181. https://doi.org/10.1016/j.marchem.2010.02.002

Song, J., Luo, Y. M., Zhao, Q. G., & Christie, P. (2003). Novel use of soil moisture samplers for studies

on anaerobic ammonium fluxes across lake sediment-water interfaces. *Chemosphere*, *50*(6), 711–715. https://doi.org/10.1016/S0045-6535(02)00210-2

Tagliabue, A., Bowie, A. R., Boyd, P. W., Buck, K. N., Johnson, K. S., & Saito, M. A. (2017). The integral role of iron in ocean biogeochemistry. *Nature*, *543*(7643), 51–59. https://doi.org/10.1038/nature21058

Tedetti, M., Cuet, P., Guigue, C., & Goutx, M. (2011). Characterization of dissolved organic matter in a coral reef ecosystem subjected to anthropogenic pressures (La Réunion Island, Indian Ocean) using multi-dimensional fluorescence spectroscopy. *Science of the Total Environment*, *409*(11), 2198–2210. https://doi.org/10.1016/j.scitotenv.2011.01.058

Terry, J. P., & Wotling, G. (2011). Rain-shadow hydrology: Influences on river flows and flood magnitudes across the central massif divide of La Grande Terre Island, New Caledonia. *Journal of Hydrology*, *404*(1–2), 77–86. https://doi.org/10.1016/j.jhydrol.2011.04.022

Thomsen, M., Dobel, S., Lassen, P., Carlsen, L., Mogensen, B. B., & Hansen, P. E. (2002). Reverse quantitative structure-activity relationship for modelling the sorption of esfenvalerate to dissolved organic matter: A multivariate approach. *Chemosphere*, *49*(10), 1317–1325. https://doi.org/10.1016/S0045-6535(02)00510-6

Thomsen, U., Thamdrup, B., Stahl, D. A., & Canfield, D. E. (2004). Pathways of organic carbon oxidation in a deep lacustrine sediment, Lake Michigan. *Limnology and Oceanography*, *49*(6), 2046–2057. https://doi.org/10.4319/lo.2004.49.6.2046

Vincent, D. G. (1994). The South Pacific Convergence Zone (SPCZ): A Review. *Monthly Weather Review*, *122*. https://doi.org/https://doi.org/10.1175/1520-0493(1994)122<1949:TSPCZA>2.0.CO;2

Wang, L., Li, H., Yang, Y., Zhang, D., Wu, M., Pan, B., & Xing, B. (2017). Identifying structural characteristics of humic acid to static and dynamic fluorescence quenching of phenanthrene, 9-phenanthrol, and naphthalene. *Water Research*, *122*, 337–344. https://doi.org/10.1016/j.watres.2017.06.010

Wang, Y., Zhang, D., Shen, Z., Feng, C., & Chen, J. (2013). Revealing Sources and Distribution Changes of Dissolved Organic Matter (DOM) in Pore Water of Sediment from the Yangtze Estuary. *PLoS ONE*, *8*(10), 11–13. https://doi.org/10.1371/journal.pone.0076633

Yamashita, Y., Maie, N., Briceño, H., & Jaffé, R. (2010). Optical characterization of dissolved organic matter in tropical rivers of the Guayana Shield, Venezuela. *Journal of Geophysical Research: Biogeosciences*, *115*(G1). https://doi.org/10.1029/2009JG000987

Zepp, R. G., Sheldon, W. M., & Moran, M. A. (2004). Dissolved organic fluorophores in southeastern US coastal waters: Correction method for eliminating Rayleigh and Raman scattering peaks in excitation-emission matrices. *Marine Chemistry*, *89*(1–4), 15–36. https://doi.org/10.1016/j.marchem.2004.02.006

Zhao, H. (2011). *Analyse de la matière organique et ses propriéetées dans l'environnement naturel en spectroscopie de fluorescence 3D traitée par PARAFAC*. Toulon.

Zhao, Y., Song, K., Wen, Z., Fang, C., Shang, Y., & Lv, L. (2017). Evaluation of CDOM sources and their links with water quality in the lakes of Northeast China using fluorescence spectroscopy. *Journal of Hydrology*, *550*, 80–91. https://doi.org/10.1016/j.jhydrol.2017.04.027

Zsolnay, A., Baigar, E., Jimenez, M., Steinweg, B., & Saccomandi, F. (1999). Differentiating with fluorescence spectroscopy the sources of dissolved organic matter in soils subjected to drying. *Chemosphere*, *38*(1), 45–50. https://doi.org/10.1016/S0045-6535(98)00166-0

1 APPENDIX

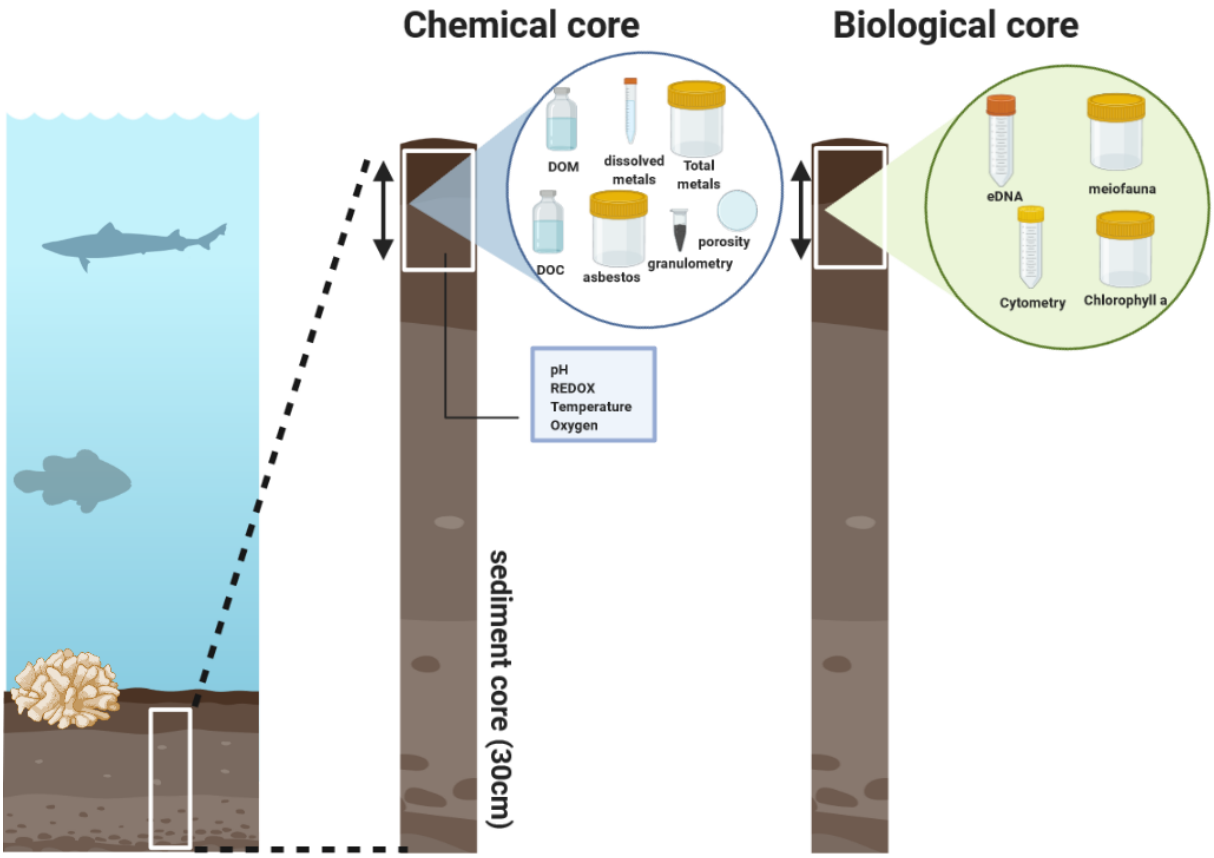

Appendix A 1: Collection of sediment samples for ECOMINE project. Two simultaneous sediments core per station. The chemical core with pore water sample (for DOM, DOC, Dissolved metals), and sediment sample (for total metal, porosity, granulometry and asbestos). The biological core with sediment sample for eDNA metabarcoding to analyse microbial communities, meiofauna, flow cytometry to analyse bacterial abundances and Chlorophyll a. Adapted from "Sediment core," by BioRender.com (2019) Retrieved from https://app.biorender.com/t-5d65983cb76ef00076060149-sediment-core

Table A1: Means ± standard deviations of in situ *physico-chemical parameters (temperature, salinity, depth, pH, Eh).*

Site	Station	Temperature	Salinity	depth	pH	Redox	Water content (%)
VKP	A	30.6	33.9	0.5	7.6 ± 0.10	-62 ± 44.1	22.36 ± 0.51
	B	31	33.6	0.7	7.4 ± 0.10	-141 ± 70.6	33.89 ± 1.69
	C	31.2	34	0.4	7.4 ± 0.11	-83 ± 16.8	59.98 ± 4.10
	D	30.5	29.6	0.3	7.2 ± 0.05	-119 ± 79.1	42.97 ± 7.01
	E	31.7	19	0.3	7.5 ± 0.05	-69 ± 14.2	42.23 ± 0.76
Ouegoa	A	29.6	29	1	7.5 ± 0.04	-56 ± 13.6	48.06 ± 2.43
	B	30.5	31.7	0.5	7.6 ± 0.09	-44 ± 41.0	25.13 ± 1.29
	C	30.7	27.7	1.2	7.4 ± 0.12	-73 ± 2.5	32.13 ± 4.93
	D	29.5	25.9	0.8	7.3 ± 0.12	-131± 27.2	57.15 ± 5.65
	E	30.2	24.5	0.6	7.5 ± 0.07	-59 ± 7.5	46.92 ± 1.44
Dumbéa	A	28.7	34.4	0.5	7.6 ± 0.03	-13 ± 55.1	25.08 ± 2.49
	B	29.2	32.5	0.7	7.3 ± 0.07	-62 ± 2.6	60.68 ± 1.96
	C	28.9	32.2	1.6	7.8 ± 0.30	-49 ± 15.0	53.92 ± 0.50
	D	28.5	33.1	1.1	7.4 ± 0.08	-58 ± 10.6	31.41 ± 0.57
	E	28.6	33.5	1.5	7.6 ± 0.14	-45 ± 11.0	31.18 ± 2.87
South of Nouméa	A	26	15	0.5	7.5 ± 0.03	-56 ± 49.2	33.87 ± 2.24
	B	28.5	31	0.6	7.7 ± 0.03	-219± 160.5	36.03 ± 4.22
	C	27.7	28.4	1	7.6 ± 0.08	-92 ± 46.9	40.52 ± 3.28
	D	26.5	22	0.9	7.7 ± 0.11	-21 ± 76.7	36.18 ± 5.59
	E	28.9	34	0.5	7.4 ± 0.20	-66 ± 107.8	29.14 ± 0.87
	F	29	22.2	0.2	7.7 ± 0.24	21 ± 51.5	37.37 ± 5.61

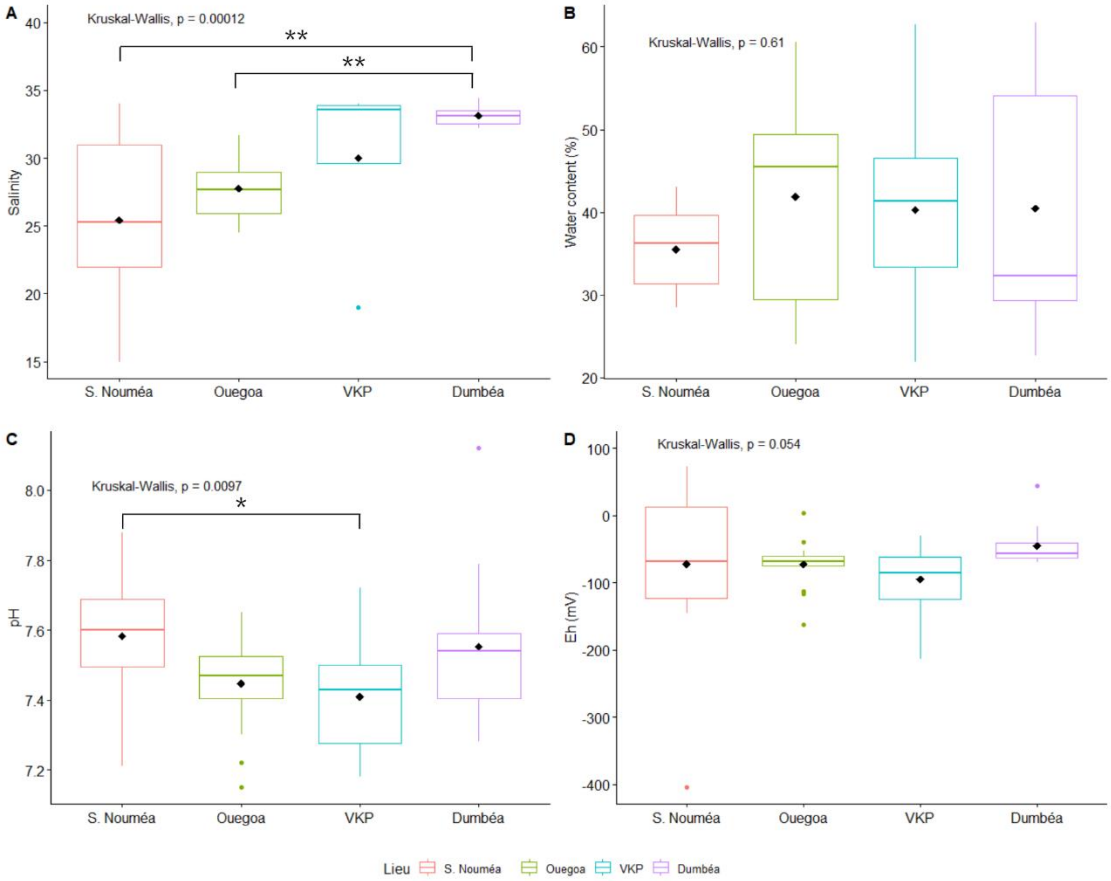

Appendix A2: Box plot illustrating inter-site variability about the different physicochemical parameters measured on the 4 sites during the ECOMINE Campaign (March-April 2022). A: Salinity, B: water content of surface sediments, C: pH, D: Eh. For the parameter's salinity and pH, the p-value of the Kruskal walis test is less than α, so we reject H0: not all medians are equal, at least one of them differs from the others. Results with p-value < 0.05 are indicated by (*) and p-value < 0.01 are indicated by (**)

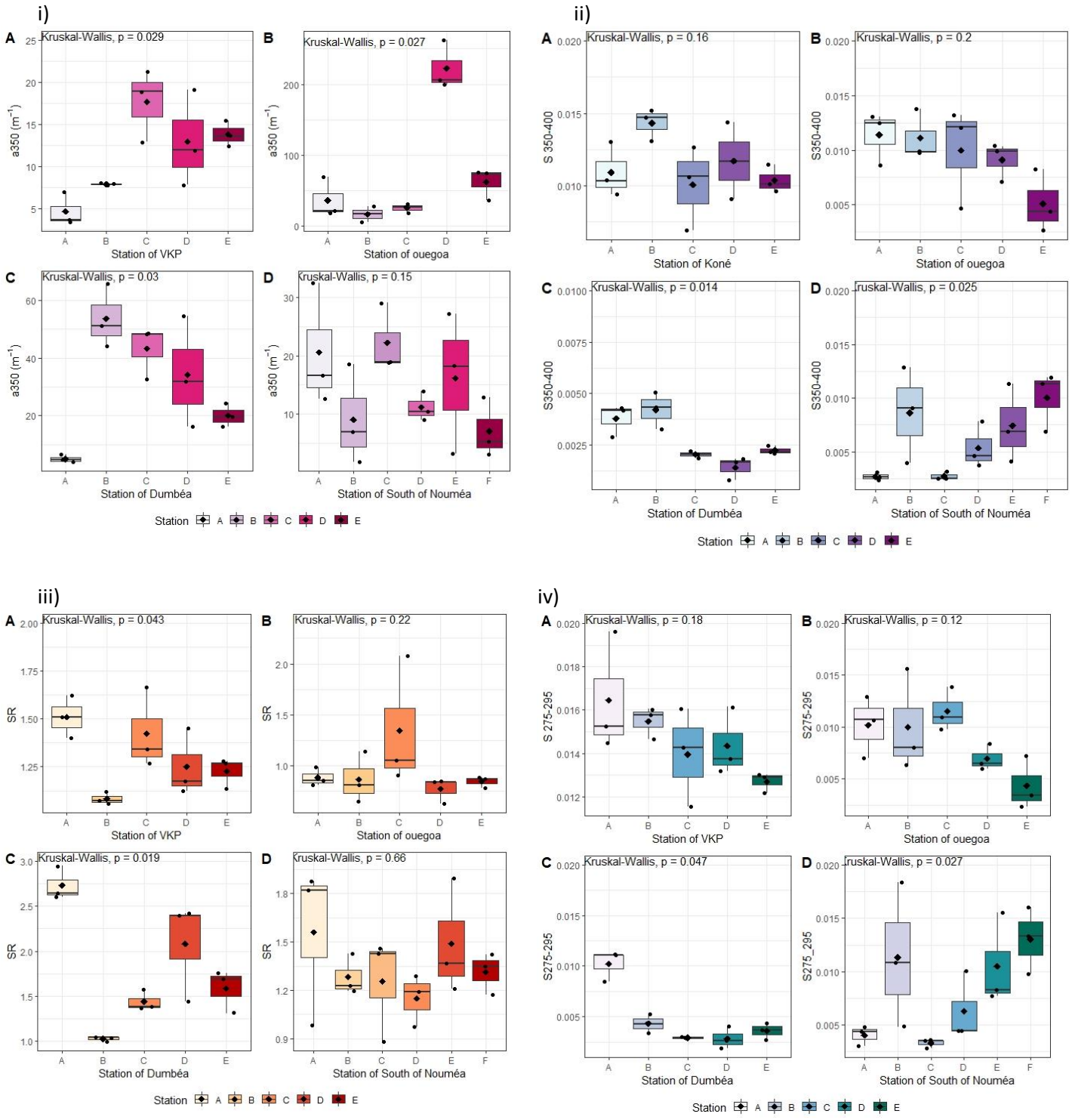

Appendix A 3 : Box plots illustrating intra-site variability about the different optical parameters measured on the 5-6 stations (A,B,C,D,E,F) and the 4 sites (VKP: A, Ouegoa: B, Dumbéa: C and D: South of Nouméa) during the ECOMINE Campaign (March-April 2022). i: a_{350} in pink, ii: $S_{350-400}$ in purple, iii: S_R in orange and iv: $S_{275-295}$ in green.

Table A 2: Means ± standard deviations (S.D.) E2/E3 and E4/E6 indices calculated in surface sediment pore waters (3cm) from VKP, Ouegoa, Dumbéa and South Nouméa sites between March and April 2022.

Site	Station	E2/E3	SD	E4/E6	SD
VKP	A	4.52	1.15	1.52	0.42
	B	4.51	0.29	7.00	1.00
	C	3.38	0.75	2.19	0.50
	D	3.72	0.70	2.37	0.45
	E	3.19	0.19	2.46	0.12
Ouegoa	A	2.91	0.78	3.40	0.49
	B	2.95	1.17	2.56	0.49
	C	3.10	0.78	2.79	0.74
	D	2.17	0.31	2.88	0.27
	E	1.58	0.44	2.55	0.37
Dumbéa	A	2.46	0.76	2.26	0.68
	B	1.42	0.11	2.68	0.15
	C	1.22	0.02	2.36	0.19
	D	1.23	0.12	2.17	0.13
	E	1.31	0.09	2.28	0.05
South of Nouméa	A	1.38	0.08	2.30	0.56
	B	3.11	1.87	2.75	0.68
	C	1.29	0.02	2.91	0.15
	D	1.90	0.53	3.14	0.41
	E	2.87	1.61	2.35	0.33
	F	3.62	1.33	2.22	0.69

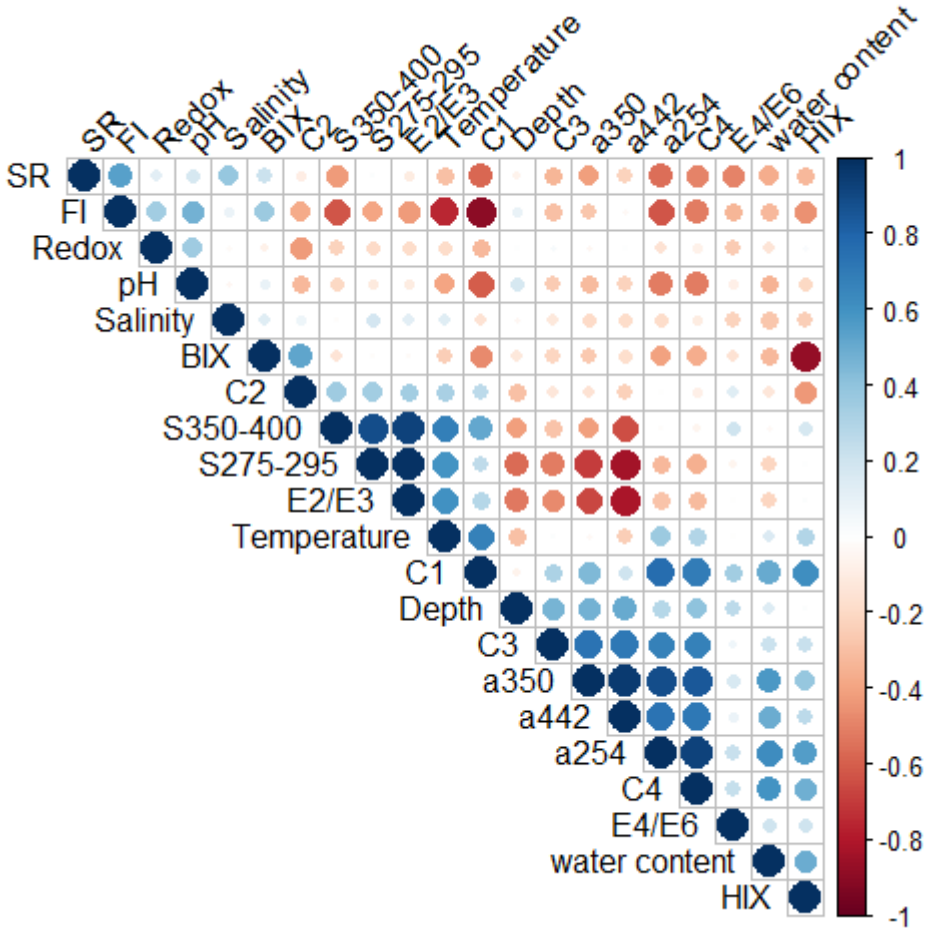

Appendix A 4: Spearman's correlation matrix of the different physico-chemical and organic matter parameters. Colour and size of the circles represent the correlation coefficients. A blue colour indicates positive correlation. and a red colour shows negative correlation.

Table A 3: Means ± standard deviations of humification (HIX) and biological production (BIX) indexes calculated in surface sediment pore waters (3cm) from the EEMS of VKP. Ouegoa. Dumbéa and South Nouméa sites between March and April 2022. Maximum of each site is shown in blue while the minimum is shown in grey.

		BIX	HIX
South of Nouméa	S-a	1.08 ± 0.08	2.85 ± 0.29
	S-b	1.13 ± 0.31	4.13 ± 1.68
	S-c	**2.81 ± 0.99**	1.07 ± 0.70
	S-d	1.04 ± 0.38	3.92 ± 2.89
	S-e	0.97 ± 0.34	5.18 ± 3.15
	S-f	0.83 ± 0.15	**8.26 ± 0.61**
Dumbéa	D-a	**1.24 ± 0.49**	1.82 ± 0.52
	D-b	0.73 ± 0.12	**9.16 ± 1.71**
	D-c	0.77 ± 0.03	6.40 ± 1.65
	D-d	0.86 ± 0.22	4.56 ± 3.06
	D-e	0.83 ± 0.11	3.48 ± 0.26
VKP	K-a	**1.50 ± 0.48**	1.53 ± 0.83
	K-b	1.32 ± 0.47	3.60 ± 2.37
	K-c	0.83 ± 0.38	**12.46 ± 11.32**
	K-d	1.29 ± 0.12	2.91 ± 0.33
	K-e	0.66 ± 0.07	9.86 ± 3.15
Ouegoa	O-a	0.62 ± 0.09	8.22 ± 1.88
	O-b	**2.12 ± 2.29**	2.63 ± 1.92
	O-c	0.71 ± 0.21	6.68 ± 2.58
	O-d	0.83 ± 0.41	**9.45 ± 6.11**
	O-e	0.94 ± 0.36	6.75 ± 4.74

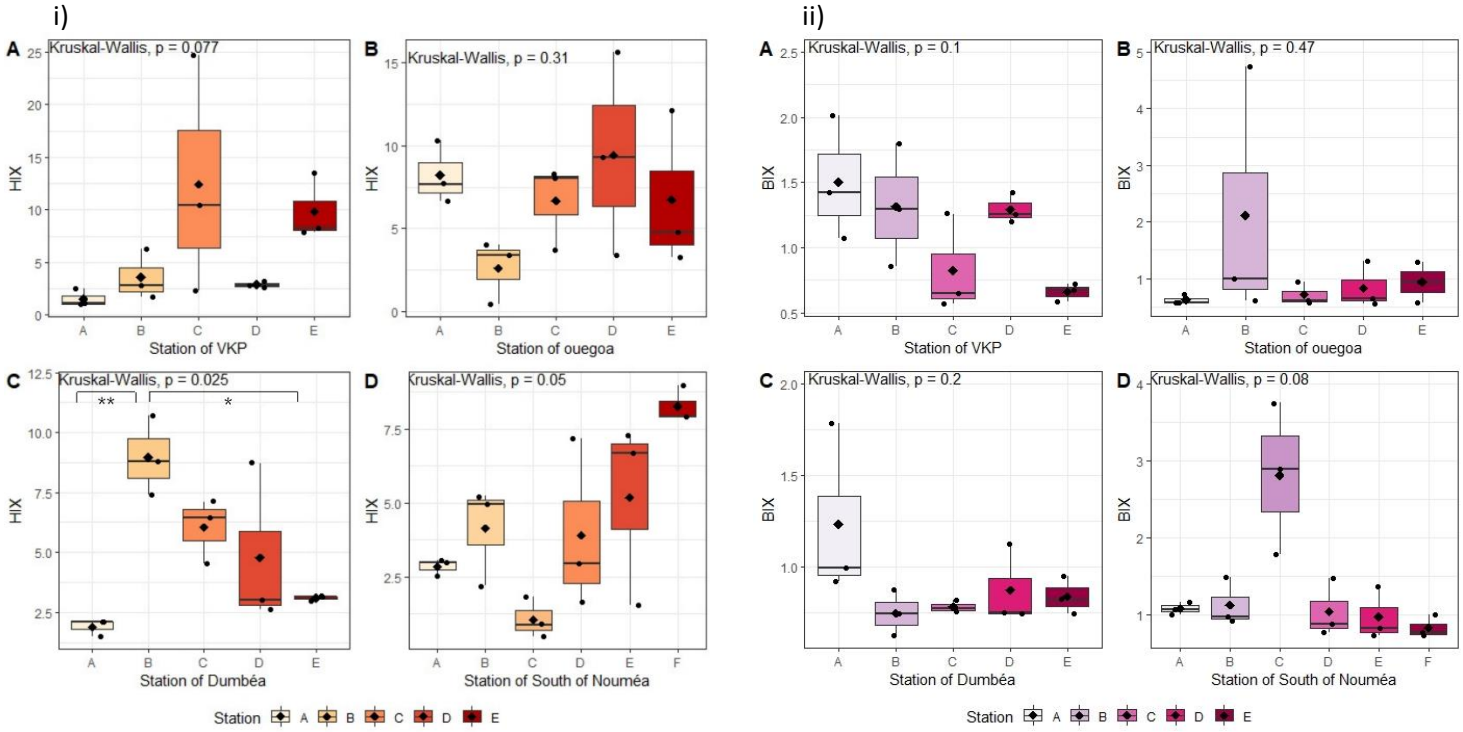

Appendix A5: Box plots illustrating intra-site variability about the HIX. and BIX indexes calculated on the 4 sites during the ECOMINE Campaign (March-April 2022). i: HIX in orange. ii: BIX in pink. The four sites are representing by dark bold letter (A.B.C.D). for both ((i) and (ii) A is for VKP. B for Ouegoa. C for Dumbéa and D for South of Nouméa. Results with p-value < 0.05 are indicated by (*) and p-value < 0.01 are indicated by (**).

Table A 4: Pseudo-concentrations (A.U) of the various fluorophores identified and validated by PARAFAC. All pseudo concentrations are expressed using arbitrary unit (A.U)

Site	Station	Humic-like	Tryptophane-like	Fulvic-acid	Terrestrial humic-like
South of Nouméa	S-a	3.25	4.38	20.94	1.73
	S-b	6.36	7.64	6.53	0.48
	S-c	3.19	18.67	12.53	1.88
	S-d	4.60	4.60	5.16	0.87
	S-e	10.89	10.74	9.70	1.72
	S-f	5.69	3.69	5.94	0.38
Dumbéa	D-a	1.86	5.22	11.80	0.63
	D-b	11.81	1.46	34.89	6.24
	D-c	8.06	1.38	36.57	5.61
	D-d	6.25	5.10	5.94	3.97
	D-e	3.13	2.59	16.86	2.34
VKP	K-a	4.51	17.05	13.43	0.04
	K-b	17.23	24.65	6.19	3.81
	K-c	19.65	14.73	3.99	3.62
	K-d	20.98	30.32	14.21	3.62
	K-e	18.14	7.81	8.47	2.32
Ouegoa	O-a	25.47	7.40	60.03	6.81
	O-b	11.29	62.28	40.57	2.04
	O-c	19.73	7.45	43.97	5.33
	O-d	39.38	18.10	68.13	25.69
	O-e	15.03	5.94	60.14	7.22